bioRxiv preprint doi: https://doi.org/10.1101/2021.10.12.464044; this version posted October 13, 2021. The copyright holder for this preprint (which was not certified by peer review) is the author/funder, who has granted bioRxiv a license to display the preprint in perpetuity. It is made available under aCC-BY 4.0 International license.

A dual endosymbiosis drives nutritional adaptation to hematophagy in the invasive tick *Hyalomma marginatum*

Marie Buysse[1,2]†*, Anna Maria Floriano[3,4]†, Yuval Gottlieb[5], Tiago Nardi[3], Francesco Comandatore[6], Emanuela Olivieri[3], Alessia Giannetto[7], Ana Palomar[8], Ben Makepeace[9], Chiara Bazzocchi[10], Alessandra Cafiso[10], Davide Sassera[3]‡* and Olivier Duron[1,2]‡*

[1] MIVEGEC (Maladies Infectieuses et Vecteurs : Ecologie, Génétique, Evolution et Contrôle), Univ. Montpellier (UM) - Centre National de la Recherche Scientifique (CNRS) - Institut pour la Recherche et le Développement (IRD), Montpellier, France

[2] Centre of Research in Ecology and Evolution of Diseases (CREES), Montpellier, France

[3] Department of Biology and Biotechnology "L. Spallanzani", University of Pavia, Pavia, Italy

[4] Faculty of Science, University of South Bohemia, České Budějovice, Czech Republic

[5] Koret School of Veterinary Medicine, The Robert H. Smith Faculty of Agriculture, Food and Environment, The Hebrew University of Jerusalem, Rehovot, Israel

[6] Department of Biomedical and Clinical Sciences L. Sacco and Pediatric Clinical Research Center, University of Milan, 20133 Milan, Italy

[7] Department of Chemical, Biological, Pharmaceutical and Environmental Sciences, University of Messina, Messina, Italy

[8] Center of Rickettsiosis and Arthropod-Borne Diseases (CRETAV), San Pedro University Hospital-Center of Biomedical Research from La Rioja (CIBIR), Logroño, Spain

[9] Institute of Infection, Veterinary & Ecological Sciences, University of Liverpool, Liverpool, United King

[10] Department of Veterinary Medicine, University of Milan, Lodi, Italy

† Co-first authors

‡ Co-lead authors

* Correspondence: marie.buysse@ird.fr; davide.sassera@unipv.it; olivier.duron@ird.fr

bioRxiv preprint doi: https://doi.org/10.1101/2021.10.12.464044; this version posted October 13, 2021. The copyright holder for this preprint (which was not certified by peer review) is the author/funder, who has granted bioRxiv a license to display the preprint in perpetuity. It is made available under aCC-BY 4.0 International license.

Abstract

Many animals are dependent on microbial partners that provide essential nutrients lacking from their diet. Ticks, whose diet consists exclusively on vertebrate blood, rely on maternally inherited bacterial symbionts to supply B vitamins. While previously studied tick species consistently harbor a single lineage of those nutritional symbionts, we evidence here that the invasive tick *Hyalomma marginatum* harbors a unique dual-partner nutritional system between an ancestral symbiont, *Francisella*, and a more recently acquired symbiont, *Midichloria*. Using metagenomics, we show that *Francisella* exhibits extensive genome erosion that endangers the nutritional symbiotic interactions: Its genome includes folate and riboflavin biosynthesis pathways but deprived functional biotin biosynthesis on account of massive pseudogenization. Co-symbiosis compensates this deficiency since the *Midichloria* genome encompasses an intact biotin operon, which was primarily acquired via lateral gene transfer from unrelated intracellular bacteria commonly infecting arthropods. Thus, in *H. marginatum*, a mosaic of co-evolved symbionts incorporating gene combinations of distant phylogenetic origins emerged to prevent the collapse of an ancestral nutritional symbiosis. Such dual endosymbiosis was never reported in other blood feeders but was recently documented in agricultural pests feeding on plant sap, suggesting that it may be a key mechanism for advanced adaptation of arthropods to specialized diets.

Keywords

Endosymbiosis, hematophagy, *Francisella*, *Midichloria*, *Hyalomma*

bioRxiv preprint doi: https://doi.org/10.1101/2021.10.12.464044; this version posted October 13, 2021. The copyright holder for this preprint (which was not certified by peer review) is the author/funder, who has granted bioRxiv a license to display the preprint in perpetuity. It is made available under aCC-BY 4.0 International license.

Introduction

Ticks evolved to hematophagy through the acquisition of key genomic adaptations (Gulia-Nuss et al., 2016; Jia et al., 2020) and the evolution of mutualistic interactions with microbial symbionts (Buysse and Duron, 2021; Duron and Gottlieb, 2020). Ticks rely on vertebrate blood as their sole food source throughout their development, although it is nutritionally unbalanced: Blood contains high levels of proteins, iron, and salts, but low levels of carbohydrates, lipids, and vitamins. To overcome these dietary challenges, tick genomes present large repertoires of genes related to vitamin and lipid shortages, iron management, and osmotic homeostasis (Gulia-Nuss et al., 2016; Jia et al., 2020). Yet, tick genomes do not contain genes for synthesis of some essential vitamins, thus vitamin-provisioning pathways have indirectly arisen from symbiotic associations with transovarially transmitted intracellular bacteria (Ben-Yosef et al., 2020; Duron et al., 2018; Duron and Gottlieb, 2020; Gerhart et al., 2016; Gottlieb et al., 2015; Guizzo et al., 2017; Smith et al., 2015). This partnership allowed the long-term acquisition of heritable biochemical functions by ticks and favored their radiation into the nearly 900 tick species that currently exist (Duron and Gottlieb, 2020). This co-evolutionary process is reflected by microbial communities dominated by tick nutritional symbionts (Bonnet and Pollet, 2020; Narasimhan and Fikrig, 2015).

Most tick species typically harbor a single lineage of nutritional symbiont, but multiple symbiont lineages exist in different tick species (Duron and Gottlieb, 2020). The most common lineages belong to the *Coxiella*-like endosymbiont group and to the *Francisella*-like endosymbiont group (CLE and FLE, hereafter) (Azagi et al., 2017; Binetruy et al., 2020; Duron et al., 2017; Machado-Ferreira et al., 2016), but a few tick species may rely on other symbionts (Duron et al., 2017), such as the intramitochondrial bacterium *Midichloria* (Sassera et al., 2006). Once deprived of their nutritional symbionts, ticks show a complete stop of

bioRxiv preprint doi: https://doi.org/10.1101/2021.10.12.464044; this version posted October 13, 2021. The copyright holder for this preprint (which was not certified by peer review) is the author/funder, who has granted bioRxiv a license to display the preprint in perpetuity. It is made available under aCC-BY 4.0 International license.

74 growth and moulting, as well as lethal physical abnormalities (Ben-Yosef et al., 2020; Duron
75 et al., 2018; Guizzo et al., 2017; Zhong et al., 2007), which can be fully restored with an
76 artificial supplement of B vitamins (Duron et al., 2018). Genomes of CLE and FLE
77 consistently contain complete biosynthesis pathways of the same three B vitamins: biotin
78 (vitamin B_7), riboflavin (B_2), and folate (B_9) (Duron et al., 2018; Gerhart et al., 2018, 2016;
79 Gottlieb et al., 2015; Guizzo et al., 2017; Nardi et al., 2021; Smith et al., 2015). These three
80 pathways form a set of core symbiotic genes essential for ticks (Duron and Gottlieb, 2020)
81 while other functions are disposable: As such, the genomes of CLE, FLE and *Midichloria*
82 underwent massive reduction as observed in other nutritional endosymbionts of arthropods
83 with a specialized diet (Duron et al., 2018; Gerhart et al., 2018, 2016; Gottlieb et al., 2015;
84 Nardi et al., 2021; Sassera et al., 2011; Smith et al., 2015). This reduction process is primarily
85 initiated as a consequence of relaxed selection on multiple genes which are not essential
86 within the host stable and nutrient-rich cellular environment (Bennett and Moran, 2015;
87 McCutcheon et al., 2019). Over time, genes encoding for functions such as motility,
88 regulation, secondary-metabolite biosynthesis, and defense are pseudogenized and then
89 definitively jettisoned (Bennett and Moran, 2015; McCutcheon et al., 2019).
90
91 Coevolution of hosts and their nutritional symbionts over millions of years is expected to
92 result in stable co-cladogenesis (Bennett and Moran, 2015). However, in sap-feeding insects
93 where symbionts compensate for nutritional deficiencies of the sap diet, cases of unstable
94 interactions have been observed (Bennett and Moran, 2015; McCutcheon et al., 2019).
95 Indeed, as the symbiont genome decays, repair mechanisms can be lost, leading to faster
96 pseudogenization, which can affect genes in all functional categories including those involved
97 in nutritional supplementation (Bennett and Moran, 2015; McCutcheon et al., 2019). This
98 may ultimately lead to overly reduced and maladapted genomes, limiting beneficial

bioRxiv preprint doi: https://doi.org/10.1101/2021.10.12.464044; this version posted October 13, 2021. The copyright holder for this preprint (which was not certified by peer review) is the author/funder, who has granted bioRxiv a license to display the preprint in perpetuity. It is made available under aCC-BY 4.0 International license.

contributions to hosts and opening the road to wholesale replacement by new symbiont(s) (Bennett and Moran, 2015; McCutcheon et al., 2019; Sudakaran et al., 2017). This degeneration–replacement model has been proposed in sap-feeding insects (Campbell et al., 2015; Łukasik et al., 2017; Manzano-Marín et al., 2020; Matsuura et al., 2018), but is difficult to document as such replacements are expected to be transient (McCutcheon et al., 2019). In parallel, other forms of multi-partite interactions have been reported, where a novel bacterium with similar function to a pre-existing symbiont enters a bipartite system (Husnik and Mccutcheon, 2016; Santos-Garcia et al., 2018; Takeshita et al., 2019). This can lead to relaxation of conservative selection pressure on the original symbionts, which can lose genes that were previously fundamental, ultimately leading to a tripartite stable symbiosis (Husnik and Mccutcheon, 2016; Takeshita et al., 2019).

In this study we document a complex nutritional endosymbiosis in the invasive bont-legged tick *Hyalomma marginatum* characterized by a maladapted ancestral symbiont genome compensated by gene functions of a more recently acquired symbiont. This large tick species usually feeds on humans and a diversity of mammals and birds in the Mediterranean climatic zone but has recently expanded its range to the north, invading Western Europe (Vial et al., 2016). *Hyalomma marginatum* can transmits Crimean-Congo hemorrhagic fever virus, an emerging disease affecting humans in the northern Mediterranean Basin, as well as protozoan parasites and intracellular bacterial pathogens such as *Rickettsia aeschlimannii* (Vial et al., 2016). Previous studies detected the presence of diverse highly prevalent bacterial symbionts across *H. marginatum* populations (Di Lecce et al., 2018), but their contribution to tick nutrition was not studied. Here we sequenced three microbial metagenomes of *H. marginatum* in three distinct locations, and determined the nutritional interactions in this unique symbiosis system.

bioRxiv preprint doi: https://doi.org/10.1101/2021.10.12.464044; this version posted October 13, 2021. The copyright holder for this preprint (which was not certified by peer review) is the author/funder, who has granted bioRxiv a license to display the preprint in perpetuity. It is made available under aCC-BY 4.0 International license.

Results

Microbial metagenomes

We sequenced three microbial metagenomes from *H. marginatum* specimens collected in Spain (i.e., the Hmar-ES metagenome), Italy (Hmar-IT), and Israel (Hmar-IL). We obtained 57,592,510 paired-end reads from the Hmar-ES metagenome, 68,515,944 paired-end reads from Hmar-IT, and 10,807,740 paired-end reads from Hmar-IL. We assembled one complete FLE genome from each metagenome (FLE-Hmar-ES, FLE-Hmar-IT, and FLE-Hmar-IL; also designated as FLE-Hmar genomes). In parallel, we assembled one complete genome from each metagenome for the bacterium *Midichloria*, and thus obtained three additional complete genomes (Midi-Hmar-ES, Midi-Hmar-IT, and Midi-Hmar-IL; also designated as Midi-Hmar genomes). In addition, we detected a third bacterium, the tick-borne pathogen *Rickettsia aeschlimannii*, in the Hmar-IT and Hmar-IL, but not Hmar-ES, metagenomes, and further assembled one complete (RAES-Hmar-IT) and one partial (RAES-Hmar-IL) genome (Figure 1).

The assemblies of the three FLE draft genomes (13 contigs for FLE Hmar-IT, 17 for FLE Hmar-ES, and 25 FLE Hmar-IL) were very similar in size (1.51 to 1.536 Mb), average G+C content (31.11 to 31.23%), number of predicted protein-coding genes (937 to 961), and protein-coding sequences with inactivating mutations (pseudogenes, 789 to 798), but no signal of mobile elements (Supplementary Table S1). Phylogenomic analysis based on 436 single-copy orthologous *Francisella* genes showed that FLE-Hmar-ES, FLE-Hmar-IT, and FLE-Hmar-IL cluster together in a robust clade within other FLE of ticks (Figure 2A). The closest relative of this clade is the FLE of another *Hyalomma* species, *Hyalomma asiaticum* from China, while FLEs of other tick genera (*Ornithodoros*, *Argas*, and *Amblyomma*) are

bioRxiv preprint doi: https://doi.org/10.1101/2021.10.12.464044; this version posted October 13, 2021. The copyright holder for this preprint (which was not certified by peer review) is the author/funder, who has granted bioRxiv a license to display the preprint in perpetuity. It is made available under aCC-BY 4.0 International license.

more distantly related. The FLE clade is embedded in the *Francisella* genus and shares a common origin with pathogenic species, including the tularemia agent, *F. tularensis*, and an opportunistic human pathogen, *F. opportunistica* (Figure 2A). The FLE-Hmar genomes are similar in organization and content overall, apart from a 127,168 bp inversion in FLE-Hmar-ES and a 4,165 bp inversion in FLE-Hmar-IL (Figure 2B). Compared to other FLE genomes (i.e. FLEOm and FLEAm), they are slightly reduced in size and exhibit substantial rearrangements (Figure 2B, Tables S1 and S2). Based on gene orthologs, the core-genome of these FLE shares 743 genes, while the core genome of the FLE of *H. marginatum* contains 796 genes because the FLE-Hmar genomes share 53 genes that are not present in other FLE genomes (Figure 2C). Interestingly, pseudogenes are highly abundant in the three genomes of FLE of *H. marginatum*, compared with other FLE genomes (Figure 2D), and most functional categories are impacted by this advanced pseudogenization process. Most of the genes associated with virulence in pathogenic *Francisella* species, including the *Francisella* Pathogenicity Island (FPI) and secretion system, are pseudogenized or completely missing in FLE-Hmar genomes, consistent with previous observations in other FLEs (Figure S1). Furthermore, FLE-Hmar genomes contain fewer genes involved in replication, recombination, and repair than any other FLEs analyzed (Figure 2C). The nucleotide excision repair system (*uvrABCD*) in FLE-Hmar genomes is conserved, however the DNA mismatch repair system (*mutSL*) is fully pseudogenized. In other FLEs, these systems are conserved, with the exception of the *mutSL* system in the FLE of *Ornithodoros moubata* and *H. asiaticum* genomes (Figure S2).

The *Midichloria* genomes, Midi-Hmar-ES, Midi-Hmar-IT, and Midi-Hmar-IL, were assembled in 179, 359 and 123 contigs respectively, and their genomes reach 1.13 to 1.16 Mb, with consistent G+C content (35.03-35.23%), number of predicted protein-coding genes

bioRxiv preprint doi: https://doi.org/10.1101/2021.10.12.464044; this version posted October 13, 2021. The copyright holder for this preprint (which was not certified by peer review) is the author/funder, who has granted bioRxiv a license to display the preprint in perpetuity. It is made available under aCC-BY 4.0 International license.

(1,032 to 1,071), pseudogenes (190 to 192), and no signal of mobile elements (Table S1). Remarkably, their average coding density (76%) is higher than those of FLEs of *H. marginatum* (54%), and furthermore, those of other FLE representatives (range from 57 to 69%). Phylogenomic analysis based on 242 single-copy orthologous *Rickettsiales* genes shows that Midi-Hmar-ES, Midi-Hmar-IT, and Midi-Hmar-IL cluster in a highly supported monophyletic sister group of the single other sequenced *Midichloria* genome, *Candidatus* M. mitochondrii strain IricVA (*M. mitochondrii* hereafter), the intra-mitochondrial endosymbiont of the European sheep tick, *Ixodes ricinus*. Altogether, they delineate a monophyletic clade within the *Midichloriaceae* family (Figure 3A). The high number of Midi-Hmar contigs precluded comparison of their genome structures. However, gene contents of the Midi-Hmar genomes are highly similar, differing substantially from *M. mitochondrii* (Tables S1 and S2). Based on gene orthologs, the pan-genome of *Midichloria* shared 745 genes, and Midi-Hmar genomes shared 181 genes that are not present in *M. mitochondrii* (Figure 3B). Pseudogenization only impacted a few functional categories (e.g., genes of chromatin structure and dynamics [category B] and genes of the mobilome [prophages and transposons, category X]), across Midi-Hmar genomes (Figure 3C). By contrast to FLE genomes, the DNA mismatch repair system (*mutSL*) and the nucleotide excision repair (*uvrABCD*) are not pseudogenized in Midi-Hmar genomes and are thus potentially functional (Figure S2).

In two metagenomes, we also detected contigs belonging to *R. aeschlimannii*. We recovered one complete chromosome (1.35 Mb for 165 contigs, with 1,122 genes, 475 pseudogenes and 32.32% G+C content) for RAES-Hmar-IT (Table S1), whereas for RAES-Hmar-IL only a partial genome (0.215 Mb) was obtained. No *Rickettsia* reads were detected in the Hmar-ES metagenome. This may be due to the absence of the bacterium in the Hmar-ES microbiome, or, possibly, to experimental artefact: This metagenome was obtained by sequencing DNA

bioRxiv preprint doi: https://doi.org/10.1101/2021.10.12.464044; this version posted October 13, 2021. The copyright holder for this preprint (which was not certified by peer review) is the author/funder, who has granted bioRxiv a license to display the preprint in perpetuity. It is made available under aCC-BY 4.0 International license.

extracted from the dissected ovaries of 10 females, whereas the Hmar-IT metagenome was sequenced from DNA extracted from a whole female, suggesting that *Rickettsia* may be absent or at low density in tick ovaries. This pattern of tissue localization may be corroborated by the Hmar-IL metagenome, sequenced from a pool of dissected ovaries of 10 ticks, but for which we obtained only a few *Rickettsia* reads. This reflects either the absence of *Rickettsia* in the dissected ticks, or a lower abundance of *Rickettsia* in ovaries. Phylogenetic analysis based on 324 single-copy orthologous genes present in *Rickettsia* genomes showed that RAES-Hmar-IT clusters with the tick-associated human pathogen *R. aeschlimannii* (including the strain MC16 previously isolated from *H. marginatum*) and altogether delineate a robust clade with the Spotted Fever *Rickettsia* group (Figure S3). Overall, the low abundance of *Rickettsia* in the Hmar-IL metagenome (8x average genome coverage), its absence in the Hmar-ES metagenome, as well as the genetic proximity with *R. aeschlimannii*, are all indicative of a tick-borne pathogen, rather than a nutritional endosymbiont. The RAES-Hmar-IT and RAES-Hmar-IL assemblies were thus not used for further analyses.

Complementation in nutritional endosymbiosis

While all previously sequenced FLE genomes contain complete pathways for biotin, riboflavin, and folate, the FLE-Hmar genomes only retain intact pathways for riboflavin and folate (Figure 4A). The biosynthesis pathway for biotin is non-functional, as from six genes of the complete pathway, one is missing and four are pseudogenized (frameshifted) in the FLE-Hmar genomes (Figure 4A). Partial biosynthesis pathways of four other B vitamins (pantothenic acid: B_5; nicotinic acid: B_3; pyridoxine: $B_{6;}$ and thiamine: B_1), each containing one to four pseudo/missing genes, are also present in the FLE-Hmar genomes; a pattern consistent with other FLE genomes (Figure S4).

bioRxiv preprint doi: https://doi.org/10.1101/2021.10.12.464044; this version posted October 13, 2021. The copyright holder for this preprint (which was not certified by peer review) is the author/funder, who has granted bioRxiv a license to display the preprint in perpetuity. It is made available under aCC-BY 4.0 International license.

The B-vitamin pathways in Midi-Hmar genomes are similar to those of *M. mitochondrii*. A complete pathway of biotin was consistently recovered in *Midichloria* genomes (Figure 4A). However, only partial pathways were detected for folate, riboflavin, and pantothenic acid with one, three, and four missing genes, respectively (Figures 4A and S4).

Ticks differ from other eukaryotes in that they lack most of the genes encoding proteins required to produce and degrade heme (Gulia-Nuss et al., 2016; Jia et al., 2020). We thus searched for relevant pathways in the symbiont genomes and found that the FLE-Hmar and Midi-Hmar genomes contain genes involved in heme and iron homeostasis. The heme biosynthetic pathway was consistently detected, as well as a gene encoding heme oxygenase that catalyzes the degradation of heme and the subsequent release of iron (Figure 4B). In these genomes we detected similar genetic patterns as those observed in the other FLE and *Midichloria* genomes. However, the heme pathway is partially degraded in FLE-Hmar genomes since their *hemN* gene is pseudogenized, a pattern not observed in other FLE genomes, suggesting an early stage of degradation for the heme pathway. This gene is present and not pseudogenized in the Midi-Hmar genomes (Figure 4B), suggesting these symbionts may compensate for the FLE heme pathway. In addition, three other genes, *hemL*, *hemY*, and *hemG* were not found in *Midichloria* genomes, but were present in FLE genomes (Figure 4B). As a result, a combination of FLE and *Midichloria* genes may be required to obtain a complete heme pathway.

Phylogenetic origins of B vitamin biosynthetic pathways

Our analysis shows that the B vitamin biosynthesis genes in the FLE-Hmar genomes have all been vertically inherited from a *Francisella* ancestor as their B vitamin genes are always more closely related to *Francisella* orthologous genes than to genes of more distantly related

bioRxiv preprint doi: https://doi.org/10.1101/2021.10.12.464044; this version posted October 13, 2021. The copyright holder for this preprint (which was not certified by peer review) is the author/funder, who has granted bioRxiv a license to display the preprint in perpetuity. It is made available under aCC-BY 4.0 International license.

bacteria (examples are shown in Figures S5A-B). Similarly, folate and riboflavin biosynthesis genes in the Midi-Hmar genomes are of *Midichloria* origin as these genes are more closely related to orthologous genes present in *M. mitochondrii* and other members of the *Midichloriaceae* family than to genes of other bacteria (Figures S5A-B).

By contrast, the six biotin genes present in the Midi-Hmar genomes did not originate from the *Midichloriaceae* family, but from an exogenous origin. The biotin synthesis genes *bioD*, *bioC*, *bioH*, *bioF*, and *bioB* formed a compact operon in the Midi-Hmar genomes while the *bioA* gene is more distantly located along the bacterial chromosome (Figure 5). A similar operon structure is also present on the *M. mitochondrii* genome. In contrast, an arrangement in which the *bioA* is gene physically associated with the remainder of the biosynthetic operon was identified on the genomes of multiple intracellular bacteria that are all distantly related to *Midichloria*, including the *Cardinium* endosymbionts (Bacteroidetes: Flexibacteraceae) of parasitoid wasps and leaf-hoppers; the *Wolbachia* endosymbionts (Alphaproteobacteria: Anaplasmataceae) of bed bugs, bees, planthoppers, and fleas; the *Legionella* endosymbiont (Gammaproteobacteria: Legionellaceae) of the rodent lice; *Rickettsia buchneri* (Alphaproteobacteria: Rickettsiaceae) symbiont of the blacklegged tick *Ixodes scapularis*; and diverse intracellular pathogens of vertebrates, such as *Lawsonia* (Deltaproteobacteria: Desulfovibrionaceae) and *Neorickettsia* (Alphaproteobacteria: Anaplasmataceae) (Figure 5 and Table S3). In most cases, the biotin genes form a compact and streamlined operon of 5-7 kb without major structural variation among bacteria. Phylogenetic analyses of the six biotin synthesis genes consistently exhibited similar evolutionary patterns (Figure 5). These patterns suggest that the biotin synthesis genes were acquired as a whole operon by an ancestor of *Midichloria* from an unrelated intracellular bacterium. In some cases, this streamlined biotin operon is also associated with nutritional symbionts of obligate blood feeders, such as

bioRxiv preprint doi: https://doi.org/10.1101/2021.10.12.464044; this version posted October 13, 2021. The copyright holder for this preprint (which was not certified by peer review) is the author/funder, who has granted bioRxiv a license to display the preprint in perpetuity. It is made available under aCC-BY 4.0 International license.

Wolbachia of bedbugs, *Legionella* of rodent lice, and *R. buchneri* in the blacklegged tick, *I. scapularis* (Figure 5).

Co-infections of nutritional endosymbionts in tick ovaries

Real-time qPCR assays on 10 field *H. marginatum* adult females indicated that FLE and *Midichloria* are both abundant in tick ovaries, with FLE and *Midichloria* detected in 10 and 9 ovarian samples, respectively. High densities were always observed for FLE (686.09 ± 206.89 FLE *rpoB* gene copies per tick *cal* gene copies) and for *Midichloria* (88.72 ± 28.41 *Midichloria gyrB* gene copies per tick *cal* gene copies) (Figure 6A). FLE were consistently most abundant with densities 5.8 to 21.4 × higher than *Midichloria* densities (paired t test, p = 0.013; one outlier was removed from analysis, n = 8). The FLE and *Midichloria* densities covaried positively in individual ticks ($\chi 2 = 23.937$, $p = 0.003$; Figure 6B).

Evolutionary history of endosymbiosis in the *Hyalomma* genus

We further examined the evolutionary history of *Hyalomma* species and their associations with FLE and *Midichloria* through a bibliographic survey. Of 10 *Hyalomma* species with sufficient published data, all were found infected by FLE, and 9 by *Midichloria* (Table S4). We next reconstructed *Hyalomma* phylogeny using mitochondrial DNA sequences of the cytochrome c oxidase I (*cox1*) gene available on Genbank (Figure S6). Mapping of FLE and *Midichloria* onto the *Hyalomma* phylogenetic tree showed that co-infection by FLE and *Midichloria* is widespread across all *Hyalomma* lineages (Figure S7). However, FLE and *Midichloria* co-infection was not detected in one species, *H. asiaticum*, nested within the *Hyalomma* phylogeny among co-infected species.

Discussion

bioRxiv preprint doi: https://doi.org/10.1101/2021.10.12.464044; this version posted October 13, 2021. The copyright holder for this preprint (which was not certified by peer review) is the author/funder, who has granted bioRxiv a license to display the preprint in perpetuity. It is made available under aCC-BY 4.0 International license.

In this study, we show that the tick *H. marginatum* is a complex symbiotic system, combining genes of diverse phylogenetic origins to generate nutritional adaptations to obligate hematophagy. This tick harbors a microbiome functionally analogous to those observed in other tick species, dominated by intracellular bacterial symbionts producing the core set of B vitamins (biotin, riboflavin, and folate) essential for tick growth and survival. However, while in other tick species, as in other obligate blood feeders, production of all three core B vitamins is performed by a single nutritional symbiont (Binetruy et al., 2020; Duron et al., 2017; Duron and Gottlieb, 2020), *H. marginatum* harbors two bacterial partners whose core B vitamins biosynthetic capacities depend on a combination of genes, with indigenous and exogenous phylogenetic origins. This multi-partner nutritional symbiosis is stably maintained at least at the tick species level, as supported by our founding of genetically similar FLE and *Midichloria* present in *H. marginatum* populations from geographically distant regions.

Genome reconstructions confirmed the key role of symbionts in *H. marginatum* nutrition, but contrary to other tick species, no single symbiont does compensate for all nutritional needs. The FLE-Hmar genomes contain the genes to synthesize folate and riboflavin but its biotin synthesis pathway is degraded, and thus non-functional. Genome reduction is a conserved trait in all FLEs, but this process has extended in the FLE of *H. marginatum*, with an additional loss of genes in most COG functional categories. This process could have been triggered by the pseudogenization of the mismatch repair system (*mutSL*), leaving the FLE of *H. marginatum* with only one DNA repair system, nucleotide excision repair (*uvrABCD*). Absence of the *mutSL* system, coupled with strict clonality and a small population size during transovarial transmission, have probably led the FLE- Hmar genomes to accumulate deleterious mutations, that resulted in maladaptation, and ultimately limited their beneficial contributions to ticks.

bioRxiv preprint doi: https://doi.org/10.1101/2021.10.12.464044; this version posted October 13, 2021. The copyright holder for this preprint (which was not certified by peer review) is the author/funder, who has granted bioRxiv a license to display the preprint in perpetuity. It is made available under aCC-BY 4.0 International license.

In the context of FLE genome degradation, co-infection with *Midichloria* prevents the breakdown and collapse of nutritional symbiosis in *H. marginatum*; i.e., the *Midichloria* genome contains an intact biotin biosynthesis operon, and thus compensates for genome decay of FLE. Inversely, *Midichloria* has only partial pathways for riboflavin and folate and hence cannot meet the nutritional needs of *H. marginatum* for these B vitamins. Consequently, the co-infection of FLE with *Midichloria* forms a cooperative system essential for the nutritional symbiosis in *H. marginatum*. In addition, complementary heme synthesis genes are present in the FLE and *Midichloria* genomes, and these symbionts may be an additional source of heme, perhaps conferring a fitness advantage to *H. marginatum* during periods of starvation. In animals, heme is essential for the function of all aerobic cells, playing an important role in controlling protein synthesis and cell differentiation. Complete biosynthetic heme gene pathways exist in most animals, but not in ticks which need an exogenous source of heme (Gulia-Nuss et al., 2016; Jia et al., 2020). Vertebrate blood is usually considered to be their unique source for this essential cofactor (Perner et al., 2016), however ticks spend most of their life off host, and thus the presence of heme genes in FLE and *Midichloria* genomes may also indicate symbiont provisioning of heme in *H. marginatum*.

The co-localization of FLE and *Midichloria* in tick ovaries suggests that vertical transmission has led to their stable co-inheritance through tick generations, linking their evolutionary fate, as observed in other symbiotic systems of arthropods (McCutcheon et al., 2019; Vautrin and Vavre, 2009). This co-transmission fidelity creates the conditions under which cooperative interactions can emerge: The stable coexistence of FLE and *Midichloria* genomes makes various genes redundant, as we observed for B vitamin and heme synthesis pathways.

bioRxiv preprint doi: https://doi.org/10.1101/2021.10.12.464044; this version posted October 13, 2021. The copyright holder for this preprint (which was not certified by peer review) is the author/funder, who has granted bioRxiv a license to display the preprint in perpetuity. It is made available under aCC-BY 4.0 International license.

Furthermore, the covariance of FLE and *Midichloria* densities in ticks is positive, suggesting that these two symbionts are not in direct competition but rather cooperative. However, while the nutritional association of FLE with *Hyalomma* species has persisted for millions of years (Azagi et al., 2017), the nutritional role of *Midichloria* seems more recent in this tick genus. Co-infection with *Midichloria* was reported in at least nine *Hyalomma* species (cf. Table S4), but in most species, such as *H. excavatum* and *H. impeltatum* (Azagi et al., 2017; Selmi et al., 2019), *Midichloria* is present at much lower frequencies than would be expected for an obligate nutritional mutualist, suggesting that it is instead a facultative (i.e., not essential) association. Interestingly, the *Hyalomma* species apparently devoid of *Midichloria*, *H. asiaticum*, harbors a FLE with intact biotin, folate, and riboflavin synthesis pathways (Buysse and Duron, 2021). In *H. marginatum*, the decay of the FLE genome may have been accelerated by the presence of *Midichloria* and the redundancy of biotin biosynthesis, a process also reported in sap-feeding insects (Husnik and Mccutcheon, 2016; Manzano-Marín et al., 2020). While it is clear that two events have led to the current status (loss of biotin genes and acquisition of *Midichloria*), the order by which these happened is unclear. *Midichloria* could have rescued a decaying symbiosis, or could have led, with its entrance in the system, to relaxation of selective constraints on FLE. Based on the common presence of *Midichloria* at lower frequencies in other *Hyalomma* species, a scenario of gradual parallel occurrence of these two events cannot be ruled out.

Our analyses also indicated that the biotin operon detected in the *Midichloria* of *H. marginatum* has an exogenous origin, being acquired following an ancient lateral gene transfer pre-dating the divergence between the *Midichloria* of *H. marginatum* and the one of *I. ricinus*. Accumulating genomic sequences indicate that this streamlined biotin operon (denoted in some studies as the Biotin synthesis Operon of Obligate intracellular Microbes –

bioRxiv preprint doi: https://doi.org/10.1101/2021.10.12.464044; this version posted October 13, 2021. The copyright holder for this preprint (which was not certified by peer review) is the author/funder, who has granted bioRxiv a license to display the preprint in perpetuity. It is made available under aCC-BY 4.0 International license.

374 BOOM (Driscoll et al., 2020)) has experienced transfers between distantly related
375 endosymbionts inhabiting arthropod cells including *Wolbachia* (Driscoll et al., 2020; Gerth
376 and Bleidorn, 2016; Ju et al., 2020; Nikoh et al., 2014), *Rickettsia* (Gillespie et al., 2012),
377 *Cardinium* (Penz et al., 2012) and *Legionella* (Říhová et al., 2017). Remarkably, the invasive
378 nature of this streamlined biotin operon has contributed not only to the emergence of novel
379 nutritional symbioses in *H. marginatum* with *Midichloria*, but also in other blood feeders,
380 such as bedbugs with *Wolbachia* (Nikoh et al., 2014) and rodent lice with *Legionella* (Říhová
381 et al., 2017), or in sap feeders as white flies with *Cardinium* (Santos-Garcia et al., 2014) and
382 planthoppers with *Wolbachia* (Ju et al., 2020). Until recently, lateral gene transfer was
383 thought to be rare in intracellular symbionts, as they reside in confined and isolated
384 environments. However, coinfections of unrelated endosymbionts within the same host cell
385 have created freely recombining intracellular bacterial communities, a unique environment
386 previously defined as the 'intracellular arena' (Kent and Bordenstein, 2010). The detection of
387 the streamlined biotin operon in *Wolbachia*, *Rickettsia*, and *Cardinium* – three of the most
388 common intracellular symbionts of arthropods (Duron et al., 2008) – corroborates the role of
389 such 'intracellular arenas' in the evolutionary dynamics of nutritional symbioses, especially as
390 the biotin operon can be found on plasmids (Gillespie et al., 2012).
391
392 The macroevolutionary and ecological consequences of acquiring nutritional symbionts are
393 immense, ticks would simply not exist as strict blood feeders without such mutualistic
394 interactions (Duron and Gottlieb, 2020). Our investigations corroborate that nutritional
395 symbionts of ticks have all converged towards an analogous process of B vitamin
396 provisioning. While past investigations showed that this evolutionary convergence consists in
397 severe degeneration of symbiont genomes accompanied by preservation of biotin, folate, and
398 riboflavin biosynthesis pathways (Buysse and Duron, 2021; Duron and Gottlieb, 2020),

bioRxiv preprint doi: https://doi.org/10.1101/2021.10.12.464044; this version posted October 13, 2021. The copyright holder for this preprint (which was not certified by peer review) is the author/funder, who has granted bioRxiv a license to display the preprint in perpetuity. It is made available under aCC-BY 4.0 International license.

399 nutritional endosymbiosis in *H. marginatum* is influenced by a more complex web of
400 interactions resulting in a dynamic mosaic of symbiont combinations and offering novel
401 evolutionary possibilities.
402

403 # Materials and Methods

404 ## Tick collection, DNA extraction and molecular screening

405 Adult females of *H. marginatum* were collected from domestic animals from three
406 geographical regions (Italy, Spain, and Israel) (Figure 1). Whole body of one female from
407 Italy was processed for metagenome sequencing, while ovaries from females collected in
408 Spain (n=10) and Israel (n=10) were used for metagenome sequencing (and for qPCR in the
409 case of samples from Spain). For each sample, total DNA was extracted using either the
410 DNeasy Blood and Tissue kit (QIAGEN) or the NucleoSpin Plant II kit (Macherey-Nagel).
411

412 A molecular screening was performed by qPCR (iQ5 system, Bio-Rad) on Spanish samples to
413 evaluate the bacterial load of FLE and *Midichloria* symbionts in ovaries. For each specimen,
414 three SYBR Green-based qPCR (Bio-Rad) assays were performed: (i) A specific
415 amplification for the *H. marginatum cal* gene, (ii) a specific amplification for the FLE *rpoB*
416 gene, and (iii) a specific amplification for the *Midichloria gyrB* gene. Thermal protocols and
417 primers are listed in Supplementary Table S5.
418

419 ## Genome sequencing, assembly and annotation

420 Metagenomes were sequenced on Illumina HiSeq 2500, after a library preparation performed
421 with Nextera XT. For the Italian and the Spanish samples, the raw paired-end reads quality
422 was evaluated with FastQC (Andrews, 2010). Paired-end reads were trimmed via
423 Trimmomatic (v0.40) (Bolger et al., 2014) and then assembled using SPAdes (v3.10.0)

bioRxiv preprint doi: https://doi.org/10.1101/2021.10.12.464044; this version posted October 13, 2021. The copyright holder for this preprint (which was not certified by peer review) is the author/funder, who has granted bioRxiv a license to display the preprint in perpetuity. It is made available under aCC-BY 4.0 International license.

(Bankevich et al., 2012) following the Blobology pipeline (Kumar et al., 2013) (thus separating reads according to G+C content, coverage, and taxonomic annotation). Discarding of contaminating sequences and refining of the assemblies were performed manually through the analysis of the assemblies' graphs with Bandage (v0.8.1) (Wick et al., 2015). Bacterial reads were separated from the tick reads, allowing the assembling of different bacterial genomes ("filtered" assemblies). For the Israeli sample, reads were trimmed using Cutadapt (v1.13) (Martin, 2011) and contaminants' reads were removed through a mapping against Coliphage phi-X174 (GenBank: NC_001422) and *Staphylococcus aureus* (NC_010079) genomes with BWA (v0.7.17-r1188) (option mem) and SAMtools (v1.10) (Li and Durbin, 2009). Remaining reads were further assembled using SPAdes (v3.11.1) (Bankevich et al., 2012) with default parameters. These "raw" assembled scaffolds were compared to different reference genomes separately (FLE of *O. moubata* FLEOm, *M. mitochondrii*, and *R. aeschlimannii*; Table S2) to discard unspecific scaffolds using RaGOO (v1.02) (Alonge et al., 2019), and, for each reference genome separately, the assignation of the remaining scaffolds ("filtered" assembly) was confirmed using the online NCBI BLAST tool (https://blast.ncbi.nlm.nih.gov/Blast.cgi). The quality assessment and the completeness of the "filtered" assemblies from all *H. marginatum* metagenomes were estimated using QUAST (v4.6.3) (Gurevich et al., 2013) and miComplete (v1.1.1) (Hugoson et al., 2020) with the --hmms Bact105 setting. The newly obtained genomes were annotated using Prokka (v1.13.1) (Seemann, 2014) with default parameters. The new *Midichloria* genomes were annotated using a manually revised annotation of *M. mitochondrii* (Table S2) as a reference.

Genomic content, structure, and metabolic pathways analyses

The FLE and *Midichloria* whole-genome alignments were obtained separately using Mauve (Darling et al., 2004). Previously, contigs from newly obtained genomes were reordered with

bioRxiv preprint doi: https://doi.org/10.1101/2021.10.12.464044; this version posted October 13, 2021. The copyright holder for this preprint (which was not certified by peer review) is the author/funder, who has granted bioRxiv a license to display the preprint in perpetuity. It is made available under aCC-BY 4.0 International license.

Mauve. Graphical representations of newly sequenced genomes were produced using CGView (v1.5) (Stothard and Wishart, 2005). Genes involved in biosynthesis pathways (B vitamins and heme), *Francisella* Pathogenecity Island (FPI), and mismatch repair systems (*mutSL* and *uvrABCD*) were retrieved using BLASTn, BLASTp, and tBLASTx on both newly obtained and reference FLE and *Midichloria* genomes. Pseudogenes prediction was performed using Pseudofinder (version downloaded in date April 1st 2020) (Syberg-Olsen et al., 2020) on each genome, including newly obtained and reference genomes of FLE and *Midichloria* (Table S2). The FLE and *Midichloria* datasets were filtered excluding pseudogenes from the subsequent analyses. Clusters of orthologous groups of proteins (COGs) were predicted using the NCBI pipeline (Galperin et al., 2015) and COGs presence was then plotted with an in-house R script. Then, two different datasets were created: (i) a FLE dataset including the three newly sequenced FLE-Hmar genomes and other published FLE genomes; and (ii) a *Midichloria* dataset including the three newly sequenced Midi-Hmar genomes and *M. mitochondrii*. For each dataset, single-copy orthologs (SCO) were identified using OrthoFinder (v2.3.12) (Emms and Kelly, 2019), then SCO lists were retrieved on a R environment (v3.6.2) to build Venn diagrams using the "VennDiagram" R package (Chen and Boutros, 2011).

Phylogenomics

The FLE, *Midichloria* and *Rickettsia* datasets were filtered excluding the pseudogene sequences and were then used for the phylogenetic analyses. For each symbiont dataset, single-copy orthologs (SCO) were identified using OrthoFinder (v2.3.12) (Emms and Kelly, 2019) and then aligned with MUSCLE (v3.8.31) (Edgar, 2004). Poorly aligned positions and divergent regions were removed by Gblocks (v0.91b) (Castresana, 2000) prior to concatenation of individual alignments using an in-house script. Finally, the most suitable

bioRxiv preprint doi: https://doi.org/10.1101/2021.10.12.464044; this version posted October 13, 2021. The copyright holder for this preprint (which was not certified by peer review) is the author/funder, who has granted bioRxiv a license to display the preprint in perpetuity. It is made available under aCC-BY 4.0 International license.

474 evolutionary model was determined using modeltest-ng (v0.1.5) (Darriba et al., 2020)
475 according to the Akaike information criterion and maximum likelihood (ML) trees were
476 inferred using RAxML (v8.2.9) (Stamatakis, 2014) with 1,000 bootstrap replicates.
477
478 **Biotin operon phylogeny and structure**
479 Nucleic and protein sequences of the six genes of the biotin biosynthesis pathway were
480 retrieved using BLASTn, BLASTp, and tBLASTx on all *Midichloria* genomes. Sequences
481 from described streamlined biotin operons and sequences from biotin genes from other
482 symbionts (retrieved from GenBank) were included in the dataset (details in Table S3). All
483 protein sequences of the six biotin genes were manually concatenated and aligned with
484 MAFFT (v7.450) (Katoh et al., 2002) and ambiguous positions were removed using trimAl
485 (v1.2rev59) (Capella-Gutiérrez et al., 2009). The appropriate substitution model, and then
486 ML-tree, were determined as described above. Meanwhile, 16S rRNA sequences from all
487 organisms included in this dataset were retrieved from GenBank and aligned with MEGA
488 software. The Gblocks program with default parameters was used to obtain non-ambiguous
489 sequence alignments. Phylogenetic analyses were performed with MEGA software, i.e.
490 determination of the appropriate substitution model using Akaike information criterion, ML-
491 tree inference. Clade robustness was assessed by bootstrap analysis using 1,000 replicates.
492
493 Contigs carrying the streamlined biotin operon were retrieved from newly obtained and
494 reference genomes of different intracellular bacteria. Contigs were annotated using Prokka
495 (v1.13.1) (Seemann, 2014) with default parameters. Prokka GenBank outputs were imported
496 in R (v3.6.2) and analyzed using the "genoplotR" R package (Guy et al., 2010). Sequences of
497 *ribH* and *folD* genes from bacteria carrying the streamlined biotin operon and from other

bioRxiv preprint doi: https://doi.org/10.1101/2021.10.12.464044; this version posted October 13, 2021. The copyright holder for this preprint (which was not certified by peer review) is the author/funder, who has granted bioRxiv a license to display the preprint in perpetuity. It is made available under aCC-BY 4.0 International license.

498 bacteria were secondarily separately analyzed. Phylogenetic analyses on these two genes were
499 performed as described above for biotin genes.
500
501 **Bibliographic survey and phylogeny of *Hyalomma***
502 To access the associations between *Hyalomma* species with FLE and *Midichloria*, we
503 performed an extensive bibliographic survey of published studies. For *Hyalomma* species for
504 which presence/absence of FLE and *Midichloria* is documented, we retrieved cytochrome c
505 oxidase I (*cox1*) gene sequences from GenBank and further performed a ML phylogenetic
506 analysis with MEGA software as described above.
507
508 **Statistical analyses**
509 Statistical analyses were carried out using the R statistical package (v3.6.2) and the "lme4" R
510 package (Bates et al., 2015). The FLE load was analyzed using linear mixed-effects models
511 on a dataset containing loads measured in ovaries from adult engorged ticks. The normality of
512 the data distribution was tested through a Shapiro-Wilk test with a 95% confidence. Outliers
513 were removed from datasets. To build models, *Midichloria* load was fitted as a fixed
514 explanatory variable. The best-fitted model was determined with the following procedure: the
515 maximal model, including all higher-order interactions, was simplified by sequentially
516 eliminating interactions and non-significant terms to establish a minimal model. A likelihood
517 ratio test (LRT) (using a chi-square distribution and a p-value cut-off of 0.05) was performed
518 to establish the difference between sequential models. The comparison between the densities
519 of FLE and *Midichloria* of *H. marginatum* was tested by a paired t test.
520
521 **Data and code availability**

bioRxiv preprint doi: https://doi.org/10.1101/2021.10.12.464044; this version posted October 13, 2021. The copyright holder for this preprint (which was not certified by peer review) is the author/funder, who has granted bioRxiv a license to display the preprint in perpetuity. It is made available under aCC-BY 4.0 International license.

The bacterial genomes obtained in this study were deposited in GenBank under accession numbers GCA_910592745 (FLE-Hmar-ES), GCA_910592815 (FLE-Hmar-IL), GCA_910592705 (FLE-Hmar-IT), GCA_910592695 (Midi-Hmar-ES), GCA_910592725 (Midi-Hmar-IL), GCA_910592865 (Midi-Hmar-IT) and GCA_910592765 (RAES-Hmar-IT). Command lines used for the different genomic analyses are available on GitHub (https://github.com/mariebuysse/Hmar-2021).

Acknowledgements

We are grateful to Tal Azagi for tick collection and extraction and Inbar Plaschkes for initial sequence analysis of the Israeli sample, to Justine Grillet, Valentina Serra and Catherine Hartley for technical support during molecular analyses. This work benefited from (1) an international 'Joint Research Projects' grant (EVOSYM) co-managed by the Ministry of Science, Technology and Space (Israel) and the Centre National de la Recherche Scientifique (CNRS, France), from (2) The Israel Science Foundation (ISF grant No. 1074/18), and from (3) the Human Frontier Science Programme Grant RGY0075/2017 to DS, and the Italian Ministry of Education, University and Research (MIUR): Dipartimenti di Eccellenza Programme (2018–2022) – Department of Biology and Biotechnology "L. Spallanzani", University of Pavia to DS.

Author contributions

D.S., Y.G. and O.D. designed the study. M.B., A.F., Y.G., D.S. and O.D. wrote the manuscript with input from other authors. M.B., A.F., T.N. and F.C. performed the genomic, phylogenomic and statistical analyses. F.C., E.O., A.G, A.P., B.M., C.B. and A.C. participated to collection and identification of specimen collection, or molecular biology. All authors agreed on the final version of the manuscript.

bioRxiv preprint doi: https://doi.org/10.1101/2021.10.12.464044; this version posted October 13, 2021. The copyright holder for this preprint (which was not certified by peer review) is the author/funder, who has granted bioRxiv a license to display the preprint in perpetuity. It is made available under aCC-BY 4.0 International license.

Competing interests

The authors declare no competing interests.

References

Alonge M, Soyk S, Ramakrishnan S, Wang X, Goodwin S, Sedlazeck FJ, Lippman ZB, Schatz MC. 2019. RaGOO: Fast and accurate reference-guided scaffolding of draft genomes. *Genome Biol* **20**:1–17. doi:10.1186/s13059-019-1829-6

Andrews S. 2010. FastQC: A quality control tool for high throughput sequence data.

Azagi T, Klement E, Perlman G, Lustig Y, Mumcuoglu KY, Apanaskevich DA, Gottlieb Y. 2017. *Francisella*-like endosymbionts and *Rickettsia* species in local and imported *Hyalomma* ticks. *Appl Environ Microbiol* **83**:1–14. doi:10.1128/AEM.01302-17

Bankevich A, Nurk S, Antipov D, Gurevich AA, Dvorkin M, Kulikov AS, Lesin VM, Nikolenko SI, Pham S, Prjibelski AD, Pyshkin A V., Sirotkin A V., Vyahhi N, Tesler G, Alekseyev MA, Pevzner PA. 2012. SPAdes: A new genome assembly algorithm and its applications to single-cell sequencing. *J Comput Biol* **19**:455–477. doi:10.1089/cmb.2012.0021

Bates D, Mächler M, Bolker BM, Walker SC. 2015. Fitting linear mixed-effects models using lme4. *J Stat Softw* **67**. doi:10.18637/jss.v067.i01

Ben-Yosef M, Rot A, Mahagna M, Kapri E, Behar A, Gottlieb Y. 2020. *Coxiella*-Like endosymbiont of *Rhipicephalus sanguineus* is required for physiological processes during ontogeny. *Front Microbiol* **11**:1–16. doi:10.3389/fmicb.2020.00493

Bennett GM, Moran NA. 2015. Heritable symbiosis : The advantages and perils of an evolutionary rabbit hole. *PNAS* **112**:10169–10176. doi:10.1073/pnas.1421388112

Binetruy F, Buysse M, Lejarre Q, Barosi R, Villa M, Rahola N, Paupy C, Ayala D, Duron O.

bioRxiv preprint doi: https://doi.org/10.1101/2021.10.12.464044; this version posted October 13, 2021. The copyright holder for this preprint (which was not certified by peer review) is the author/funder, who has granted bioRxiv a license to display the preprint in perpetuity. It is made available under aCC-BY 4.0 International license.

572 2020. Microbial community structure reveals instability of nutritional symbiosis during
573 the evolutionary radiation of *Amblyomma* ticks. *Mol Ecol* **29**:1016–1029.
574 doi:10.1111/mec.15373
575 Bolger AM, Lohse M, Usadel B. 2014. Trimmomatic: A flexible trimmer for Illumina
576 sequence data. *Bioinformatics* **30**:2114–2120. doi:10.1093/bioinformatics/btu170
577 Bonnet SI, Pollet T. 2020. Update on the intricate tango between tick microbiomes and tick-
578 borne pathogens. *Parasite Immunol* 1–12. doi:10.1111/pim.12813
579 Buysse M, Duron O. 2021. Evidence that microbes identified as tick-borne pathogens are
580 nutritional endosymbionts. *Cell*.
581 Campbell MA, Leuven JT Van, Meister RC, Carey KM, Simon C, Mccutcheon JP. 2015.
582 Genome expansion via lineage splitting and genome reduction in the cicada
583 endosymbiont *Hodgkinia*. *PNAS* **112**:10192–10199. doi:10.1073/pnas.1421386112
584 Capella-Gutiérrez S, Silla-Martínez JM, Gabaldón T. 2009. trimAl: A tool for automated
585 alignment trimming in large-scale phylogenetic analyses. *Bioinformatics* **25**:1972–1973.
586 doi:10.1093/bioinformatics/btp348
587 Castresana J. 2000. Selection of conserved blocks from multiple alignments for their use in
588 phylogenetic analysis. *Mol Biol Evol* **17**:540–552.
589 doi:10.1093/oxfordjournals.molbev.a026334
590 Chen H, Boutros PC. 2011. VennDiagram: A package for the generation of highly-
591 customizable Venn and Euler diagrams in R. *BMC Bioinformatics* **12**.
592 doi:10.2307/2689606
593 Darling ACE, Mau B, Blattner FR, Perna NT. 2004. Mauve: Multiple alignment of conserved
594 genomic sequence with rearrangements. *Genome Res* **14**:1394–1403.
595 doi:10.1101/gr.2289704
596 Darriba Di, Posada D, Kozlov AM, Stamatakis A, Morel B, Flouri T. 2020. ModelTest-NG:

bioRxiv preprint doi: https://doi.org/10.1101/2021.10.12.464044; this version posted October 13, 2021. The copyright holder for this preprint (which was not certified by peer review) is the author/funder, who has granted bioRxiv a license to display the preprint in perpetuity. It is made available under aCC-BY 4.0 International license.

597 A new and scalable tool for the selection of DNA and protein evolutionary models. *Mol*
598 *Biol Evol* **37**:291–294. doi:10.1093/molbev/msz189
599 Di Lecce I, Bazzocchi C, Cecere JG, Epis S, Sassera D, Villani BM, Bazzi G, Negri A, Saino
600 N, Spina F, Bandi C, Rubolini D. 2018. Patterns of *Midichloria* infection in avian-borne
601 African ticks and their trans-Saharan migratory hosts. *Parasites and Vectors* **11**:1–11.
602 doi:10.1186/s13071-018-2669-z
603 Driscoll TP, Verhoeve VI, Brockway C, Shrewsberry DL, Plumer M, Sevdalis SE, Beckmann
604 JF, Krueger LM, Macaluso KR, Azad AF, Gillespie JJ. 2020. Evolution of *Wolbachia*
605 mutualism and reproductive parasitism: Insight from two novel strains that co-infect cat
606 fleas. *PeerJ* **8**:1–39. doi:10.7717/peerj.10646
607 Duron O, Binetruy F, Noel V, Cremaschi J, McCoy K, Arnathau C, Plantard O, Goolsby J,
608 Perez De Leon AA, Heylen DJA, Raoul Van Oosten A, Gottlieb Y, Baneth G,
609 Guglielmone AA, Estrada-Pena A, Opara MN, Zenner L, Vavre F, Chevillon C. 2017.
610 Evolutionary changes in symbiont community structure in ticks. *Mol Ecol* **26**:2905–
611 2921. doi:10.1111/mec.14094
612 Duron O, Bouchon D, Boutin S, Bellamy L, Zhou L, Engelstadter J, Hurst GD. 2008. The
613 diversity of reproductive parasites among arthropods: *Wolbachia* do not walk alone.
614 *BMC Biol* **6**:1–12. doi:10.1186/1741-7007-6-27
615 Duron O, Gottlieb Y. 2020. Convergence of nutritional symbioses in obligate blood-feeders.
616 *Trends Parasitol*. doi:10.1016/j.pt.2020.07.007
617 Duron O, Morel O, Noël V, Buysse M, Binetruy F, Lancelot R, Loire E, Ménard C, Bouchez
618 O, Vavre F, Vial L. 2018. Tick-bacteria mutualism depends on B vitamin synthesis
619 pathways. *Curr Biol* **28**:1–7. doi:10.1016/j.cub.2018.04.038
620 Edgar RC. 2004. MUSCLE: Multiple sequence alignment with high accuracy and high
621 throughput. *Nucleic Acids Res* **32**:1792–1797. doi:10.1093/nar/gkh340

bioRxiv preprint doi: https://doi.org/10.1101/2021.10.12.464044; this version posted October 13, 2021. The copyright holder for this preprint (which was not certified by peer review) is the author/funder, who has granted bioRxiv a license to display the preprint in perpetuity. It is made available under aCC-BY 4.0 International license.

622 Emms DM, Kelly S. 2019. OrthoFinder: Phylogenetic orthology inference for comparative
623 genomics. *Genome Biol* **20**:1–14. doi:10.1186/s13059-019-1832-y
624 Galperin MY, Makarova KS, Wolf YI, Koonin E V. 2015. Expanded microbial genome
625 coverage and improved protein family annotation in the COG database. *Nucleic Acids*
626 *Res* **43**:D261–D269. doi:10.1093/nar/gku1223
627 Gerhart JG, Auguste Dutcher H, Brenner AE, Moses AS, Grubhoffer L, Raghavan R. 2018.
628 Multiple acquisitions of pathogen-derived *Francisella* endosymbionts in soft ticks.
629 *Genome Biol Evol* **10**:607–615. doi:10.1093/gbe/evy021
630 Gerhart JG, Moses AS, Raghavan R. 2016. A *Francisella*-like endosymbiont in the Gulf
631 Coast tick evolved from a mammalian pathogen. *Sci Rep* **6**:1–6. doi:10.1038/srep33670
632 Gerth M, Bleidorn C. 2016. Comparative genomics provides a timeframe for *Wolbachia*
633 evolution and exposes a recent biotin synthesis operon transfer. *Nat Microbiol* **2**.
634 doi:10.1038/nmicrobiol.2016.241
635 Gillespie JJ, Joardar V, Williams KP, Driscoll T, Hostetler JB, Nordberg E, Shukla M,
636 Walenz B, Hill CA, Nene VM, Azad AF, Sobral BW, Caler E. 2012. A *Rickettsia*
637 genome overrun by mobile genetic elements provides insight into the acquisition of
638 genes characteristic of an obligate intracellular lifestyle. *J Bacteriol* **194**:376–394.
639 doi:10.1128/JB.06244-11
640 Gottlieb Y, Lalzar I, Klasson L. 2015. Distinctive genome reduction rates revealed by
641 genomic analyses of two *Coxiella*-like endosymbionts in ticks. *Genome Biol Evol*
642 **7**:1779–1796. doi:10.1093/gbe/evv108
643 Guizzo MG, Parizi LF, Nunes RD, Schama R, Albano RM, Tirloni L, Oldiges DP, Vieira RP,
644 Oliveira WHC, Leite MDS, Gonzales SA, Farber M, Martins O, Vaz IDS, Oliveira PL.
645 2017. A *Coxiella* mutualist symbiont is essential to the development of *Rhipicephalus*
646 *microplus*. *Sci Rep* **7**:1–10. doi:10.1038/s41598-017-17309-x

bioRxiv preprint doi: https://doi.org/10.1101/2021.10.12.464044; this version posted October 13, 2021. The copyright holder for this preprint (which was not certified by peer review) is the author/funder, who has granted bioRxiv a license to display the preprint in perpetuity. It is made available under aCC-BY 4.0 International license.

647 Gulia-Nuss M, Nuss AB, Meyer JM, Sonenshine DE, Roe RM, Waterhouse RM, Sattelle DB,
648 De La Fuente J, Ribeiro JM, Megy K, Thimmapuram J, Miller JR, Walenz BP, Koren S,
649 Hostetler JB, Thiagarajan M, Joardar VS, Hannick LI, Bidwell S, Hammond MP, Young
650 S, Zeng Q, Abrudan JL, Almeida FC, Ayllón N, Bhide K, Bissinger BW, Bonzon-
651 Kulichenko E, Buckingham SD, Caffrey DR, Caimano MJ, Croset V, Driscoll T, Gilbert
652 D, Gillespie JJ, Giraldo-Calderón GI, Grabowski JM, Jiang D, Khalil SMS, Kim D,
653 Kocan KM, Koči J, Kuhn RJ, Kurtti TJ, Lees K, Lang EG, Kennedy RC, Kwon H,
654 Perera R, Qi Y, Radolf JD, Sakamoto JM, Sánchez-Gracia A, Severo MS, Silverman N,
655 Šimo L, Tojo M, Tornador C, Van Zee JP, Vázquez J, Vieira FG, Villar M, Wespiser
656 AR, Yang Y, Zhu J, Arensburger P, Pietrantonio P V., Barker SC, Shao R, Zdobnov EM,
657 Hauser F, Grimmelikhuijzen CJP, Park Y, Rozas J, Benton R, Pedra JHF, Nelson DR,
658 Unger MF, Tubio JMC, Tu Z, Robertson HM, Shumway M, Sutton G, Wortman JR,
659 Lawson D, Wikel SK, Nene VM, Fraser CM, Collins FH, Birren B, Nelson KE, Caler E,
660 Hill CA. 2016. Genomic insights into the *Ixodes scapularis* tick vector of Lyme disease.
661 *Nat Commun* **7**. doi:10.1038/ncomms10507
662 Gurevich A, Saveliev V, Vyahhi N, Tesler G. 2013. QUAST: Quality assessment tool for
663 genome assemblies. *Bioinformatics* **29**:1072–1075. doi:10.1093/bioinformatics/btt086
664 Guy L, Kultima JR, Andersson SGE, Quackenbush J. 2010. GenoPlotR: comparative gene
665 and genome visualization in R. *Bioinformatics* **27**:2334–2335.
666 doi:10.1093/bioinformatics/btq413
667 Hugoson E, Lam WT, Guy L. 2020. MiComplete: Weighted quality evaluation of assembled
668 microbial genomes. *Bioinformatics* **36**:936–937. doi:10.1093/bioinformatics/btz664
669 Husnik F, Mccutcheon JP. 2016. Repeated replacement of an intrabacterial symbiont in the
670 tripartite nested mealybug symbiosis. *PNAS* 5416–5424. doi:10.1101/042267
671 Jia N, Wang J, Shi W, Du L, Sun Y, Zhan W, Jiang JF, Wang Q, Zhang B, Ji P, Bell-Sakyi L,

bioRxiv preprint doi: https://doi.org/10.1101/2021.10.12.464044; this version posted October 13, 2021. The copyright holder for this preprint (which was not certified by peer review) is the author/funder, who has granted bioRxiv a license to display the preprint in perpetuity. It is made available under aCC-BY 4.0 International license.

672 Cui XM, Yuan TT, Jiang BG, Yang WF, Lam TTY, Chang QC, Ding SJ, Wang XJ, Zhu
673 JG, Ruan XD, Zhao L, Wei J Te, Ye RZ, Que TC, Du CH, Zhou YH, Cheng JX, Dai PF,
674 Guo W Bin, Han XH, Huang EJ, Li LF, Wei W, Gao YC, Liu JZ, Shao HZ, Wang X,
675 Wang CC, Yang TC, Huo QB, Li W, Chen HY, Chen SE, Zhou LG, Ni XB, Tian JH,
676 Sheng Y, Liu T, Pan YS, Xia LY, Li J, Zhao F, Cao WC. 2020. Large-scale comparative
677 analyses of tick genomes elucidate their genetic diversity and vector capacities. *Cell*
678 **182**:1328-1340.e13. doi:10.1016/j.cell.2020.07.023
679 Ju JF, Bing XL, Zhao DS, Guo Y, Xi Z, Hoffmann AA, Zhang KJ, Huang HJ, Gong JT,
680 Zhang X, Hong XY. 2020. *Wolbachia* supplement biotin and riboflavin to enhance
681 reproduction in planthoppers. *ISME J* **14**:676–687. doi:10.1038/s41396-019-0559-9
682 Katoh K, Misawa K, Kuma KI, Miyata T. 2002. MAFFT: A novel method for rapid multiple
683 sequence alignment based on fast Fourier transform. *Nucleic Acids Res* **30**:3059–3066.
684 doi:10.1093/nar/gkf436
685 Kent BN, Bordenstein SR. 2010. Phage WO of *Wolbachia*: Lambda of the endosymbiont
686 world. *Trends Microbiol* **18**:173–181. doi:10.1016/j.tim.2009.12.011
687 Kumar S, Jones M, Koutsovoulos G, Clarke M, Blaxter M. 2013. Blobology: exploring raw
688 genome data for contaminants, symbionts and parasites using taxon-annotated GC-
689 coverage plots. *Front Genet* **4**:1–12. doi:10.3389/fgene.2013.00237
690 Li H, Durbin R. 2009. Fast and accurate short read alignment with Burrows-Wheeler
691 transform. *Bioinformatics* **25**:1754–1760. doi:10.1093/bioinformatics/btp324
692 Łukasik P, Nazario K, Van Leuven JT, Campbell MA, Meyer M, Michalik A, Pessacq P,
693 Simon C, Veloso C, McCutcheon JP. 2017. Multiple origins of interdependent
694 endosymbiotic complexes in a genus of cicadas. *Proc Natl Acad Sci U S A* **115**:E226–
695 E235. doi:10.1073/pnas.1712321115
696 Machado-Ferreira E, Vizzoni VF, Balsemao-Pires E, Moerbeck L, Gazeta GS, Piesman J,

bioRxiv preprint doi: https://doi.org/10.1101/2021.10.12.464044; this version posted October 13, 2021. The copyright holder for this preprint (which was not certified by peer review) is the author/funder, who has granted bioRxiv a license to display the preprint in perpetuity. It is made available under aCC-BY 4.0 International license.

697 Voloch CM, Soares CAG. 2016. *Coxiella* symbionts are widespread into hard ticks.
698 *Parasitol Res* **115**:4691–4699. doi:10.1007/s00436-016-5230-z
699 Manzano-Marín A, Coeur d'acier A, Clamens AL, Orvain C, Cruaud C, Barbe V, Jousselin E.
700 2020. Serial horizontal transfer of vitamin-biosynthetic genes enables the establishment
701 of new nutritional symbionts in aphids' di-symbiotic systems. *ISME J* **14**:259–273.
702 doi:10.1038/s41396-019-0533-6
703 Martin M. 2011. Cutadapt removes adapter sequences from high-throughput sequencing
704 reads. *EMBnet.journal* **17**:10–12. doi:doi.org/10.14806/ej.17.1.200
705 Matsuura Y, Moriyama M, Łukasik P, Vanderpool D, Tanahashi M, Meng XY, McCutcheon
706 JP, Fukatsu T. 2018. Recurrent symbiont recruitment from fungal parasites in cicadas.
707 *Proc Natl Acad Sci U S A* **115**:E5970–E5979. doi:10.1073/pnas.1803245115
708 McCutcheon JP, Boyd BM, Dale C. 2019. The life of an insect endosymbiont from the cradle
709 to the grave. *Curr Biol* **29**:485–495. doi:10.1016/j.cub.2019.03.032
710 Narasimhan S, Fikrig E. 2015. Tick microbiome: The force within. *Trends Parasitol* **31**:315–
711 323. doi:10.1016/j.pt.2015.03.010
712 Nardi T, Olivieri E, Kariuki E, Sassera D, Castelli M. 2021. Sequence of a *Coxiella*
713 endosymbiont of the tick *Amblyomma nuttalli* suggests a pattern of convergent genome
714 reduction in the *Coxiella* genus. *Genome Biol Evol* **13**:1–7. doi:10.1093/gbe/evaa253
715 Nikoh N, Hosokawa T, Moriyama M, Oshima K, Hattori M, Fukatsu T. 2014. Evolutionary
716 origin of insect-*Wolbachia* nutritional mutualism. *Proc Natl Acad Sci U S A* **111**:10257–
717 10262. doi:10.1073/pnas.1409284111
718 Penz T, Schmitz-Esser S, Kelly SE, Cass BN, Müller A, Woyke T, Malfatti SA, Hunter MS,
719 Horn M. 2012. Comparative genomics suggests an independent origin of cytoplasmic
720 incompatibility in *Cardinium hertigii*. *PLoS Genet* **8**. doi:10.1371/journal.pgen.1003012
721 Perner J, Sobotka R, Sima R, Konvickova J, Sojka D, de Oliveira PL, Hajdusek O, Kopacek

bioRxiv preprint doi: https://doi.org/10.1101/2021.10.12.464044; this version posted October 13, 2021. The copyright holder for this preprint (which was not certified by peer review) is the author/funder, who has granted bioRxiv a license to display the preprint in perpetuity. It is made available under aCC-BY 4.0 International license.

722 P. 2016. Acquisition of exogenous haem is essential for tick reproduction. *Elife* **5**:1–20.
723 doi:10.7554/eLife.12318
724 Říhová J, Novaková E, Husník F, Hypša V. 2017. *Legionella* becoming a mutualist: Adaptive
725 processes shaping the genome of symbiont in the louse *Polyplax serrata*. *Genome Biol*
726 *Evol* **9**:2946–2957. doi:10.1093/gbe/evx217
727 Santos-Garcia D, Rollat-Farnier PA, Beitia F, Zchori-Fein E, Vavre F, Mouton L, Moya A,
728 Latorre A, Silva FJ. 2014. The genome of *Cardinium* cBtQ1 provides insights into
729 genome reduction, symbiont motility, and its settlement in *Bemisia tabaci*. *Genome Biol*
730 *Evol* **6**:1013–1030. doi:10.1093/gbe/evu077
731 Santos-Garcia Di, Juravel K, Freilich S, Zchori-Fein E, Latorre A, Moya A, Morin S, Silva
732 FJ. 2018. To B or not to B: Comparative genomics suggests *Arsenophonus* as a source of
733 B vitamins in whiteflies. *Front Microbiol* **9**:1–16. doi:10.3389/fmicb.2018.02254
734 Sassera D, Beninati T, Bandi C, Bouman EAP, Sacchi L, Fabbi M, Lo N. 2006. *Candidatus*
735 Midichloria mitochondrii', an endosymbiont of the *Ixodes ricinus* with a unique
736 intramitochondrial lifestyle. *Int J Syst Evol Microbiol* **56**:2535–2540.
737 doi:10.1099/ijs.0.64386-0
738 Sassera D, Lo N, Epis S, D'Auria G, Montagna M, Comandatore F, Horner D, Peretó J,
739 Luciano AM, Franciosi F, Ferri E, Crotti E, Bazzocchi C, Daffonchio D, Sacchi L, Moya
740 A, Latorre A, Bandi C. 2011. Phylogenomic evidence for the presence of a flagellum and
741 *cbb3* oxidase in the free-living mitochondrial ancestor. *Mol Biol Evol* **28**:3285–3296.
742 doi:10.1093/molbev/msr159
743 Seemann T. 2014. Prokka: Rapid prokaryotic genome annotation. *Bioinformatics* **30**:2068–
744 2069. doi:10.1093/bioinformatics/btu153
745 Selmi R, Ben Said M, Mamlouk A, Ben Yahia H, Messadi L. 2019. Molecular detection and
746 genetic characterization of the potentially pathogenic *Coxiella burnetii* and the

bioRxiv preprint doi: https://doi.org/10.1101/2021.10.12.464044; this version posted October 13, 2021. The copyright holder for this preprint (which was not certified by peer review) is the author/funder, who has granted bioRxiv a license to display the preprint in perpetuity. It is made available under aCC-BY 4.0 International license.

endosymbiotic *Candidatus* Midichloria mitochondrii in ticks infesting camels (*Camelus dromedarius*) from Tunisia. *Microb Pathog* **136**:103655. doi:10.1016/j.micpath.2019.103655

Smith TA, Driscoll T, Gillespie JJ, Raghavan R. 2015. A *Coxiella*-like endosymbiontis a potential vitamin source for the lone star tick. *Genome Biol Evol* **7**:831–838. doi:10.1093/gbe/evv016

Stamatakis A. 2014. RAxML version 8: A tool for phylogenetic analysis and post-analysis of large phylogenies. *Bioinformatics* **30**:1312–1313. doi:10.1093/bioinformatics/btu033

Stothard P, Wishart DS. 2005. Circular genome visualization and exploration using CGView. *Bioinformatics* **21**:537–539. doi:10.1093/bioinformatics/bti054

Sudakaran S, Kost C, Kaltenpoth M. 2017. Symbiont acquisition and replacement as a source of ecological innovation. *Trends Microbiol*. doi:10.1016/j.tim.2017.02.014

Syberg-Olsen M, Garber A, Keeling P, McCutcheon J, Husnik F. 2020. Pseudofinder.

Takeshita K, Yamada T, Kawahara Y, Narihiro T, Ito M, Kamagata Y, Shinzato N. 2019. Tripartite symbiosis of an anaerobic scuticociliate with two hydrogenosome-associtaed endosymbionts, a *Holospora*-related alphaproteobacterium and a methanogenic archaeon. *Appl Environ Microbiol* **7**:1–14.

Vautrin E, Vavre F. 2009. Interactions between vertically transmitted symbionts: cooperation or conflict? *Trends Microbiol* **17**:95–99. doi:10.1016/j.tim.2008.12.002

Vial L, Stachurski F, Leblond A, Huber K, Vourc'h G, René-Martellet M, Desjardins I, Balança G, Grosbois V, Pradier S, Gély M, Appelgren A, Estrada-Peña A. 2016. Strong evidence for the presence of the tick *Hyalomma marginatum* Koch, 1844 in southern continental France. *Ticks Tick Borne Dis* **7**:1162–1167. doi:10.1016/j.ttbdis.2016.08.002

Wick RR, Schultz MB, Zobel J, Holt KE. 2015. Bandage: Interactive visualization of *de novo* genome assemblies. *Bioinformatics* **31**:3350–3352. doi:10.1093/bioinformatics/btv383

bioRxiv preprint doi: https://doi.org/10.1101/2021.10.12.464044; this version posted October 13, 2021. The copyright holder for this preprint (which was not certified by peer review) is the author/funder, who has granted bioRxiv a license to display the preprint in perpetuity. It is made available under aCC-BY 4.0 International license.

772 Zhong J, Jasinskas A, Barbour AG. 2007. Antibiotic treatment of the tick vector *Amblyomma*

773 *americanum* reduced reproductive fitness. *PLoS One* **2**:1–7.

774 doi:10.1371/journal.pone.0000405

775

bioRxiv preprint doi: https://doi.org/10.1101/2021.10.12.464044; this version posted October 13, 2021. The copyright holder for this preprint (which was not certified by peer review) is the author/funder, who has granted bioRxiv a license to display the preprint in perpetuity. It is made available under aCC-BY 4.0 International license.

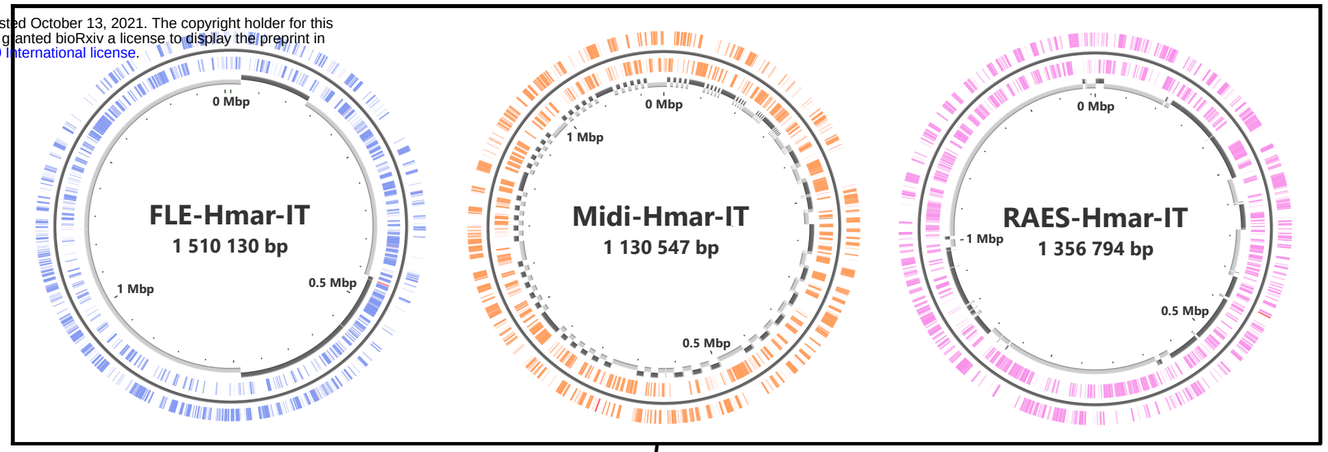

Genomes' legends

Francisella	*Midichloria*	*Rickettsia*
CDS	CDS	CDS
tRNA	tRNA	tRNA
rRNA	rRNA	rRNA
Other	Other	Other

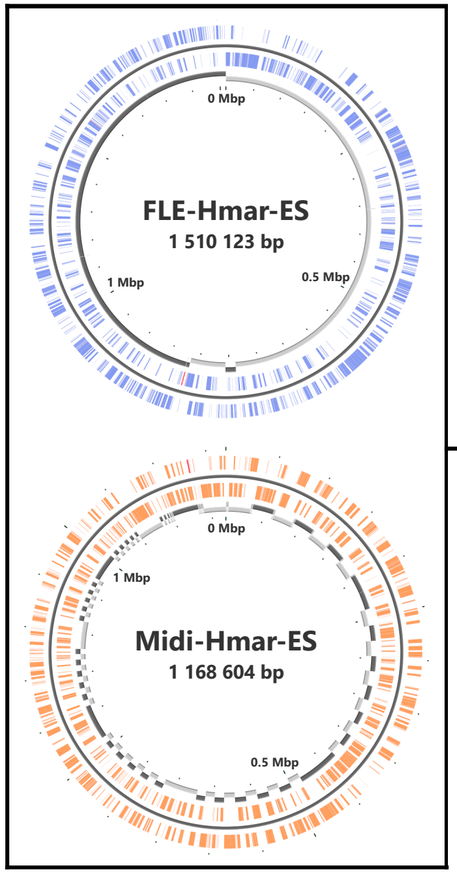

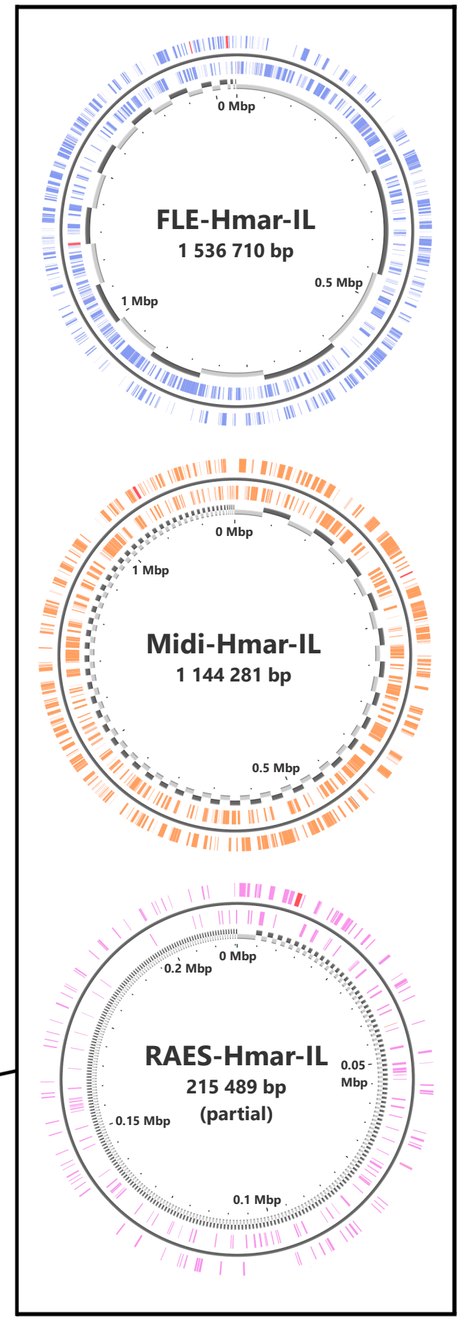

bioRxiv preprint doi: https://doi.org/10.1101/2021.10.12.464044; this version posted October 13, 2021. The copyright holder for this preprint (which was not certified by peer review) is the author/funder, who has granted bioRxiv a license to display the preprint in perpetuity. It is made available under aCC-BY 4.0 International license.

Figure 1. Sampled locations for *H. marginatum* ticks. Sampling countries are colored in grey. The symbiont genomes retrieved from each site are graphically represented in blue, orange and pink, corresponding to *Francisella*-LE (FLE), *Midichloria* (Midi) and *R. aeschlimannii* (RAES), respectively. Circles on genome maps correspond to the following: (1) forward strand genes; (2) reverse strand genes, (3) in grey and black, contigs. Circular maps of the genomes were produced using CGView.

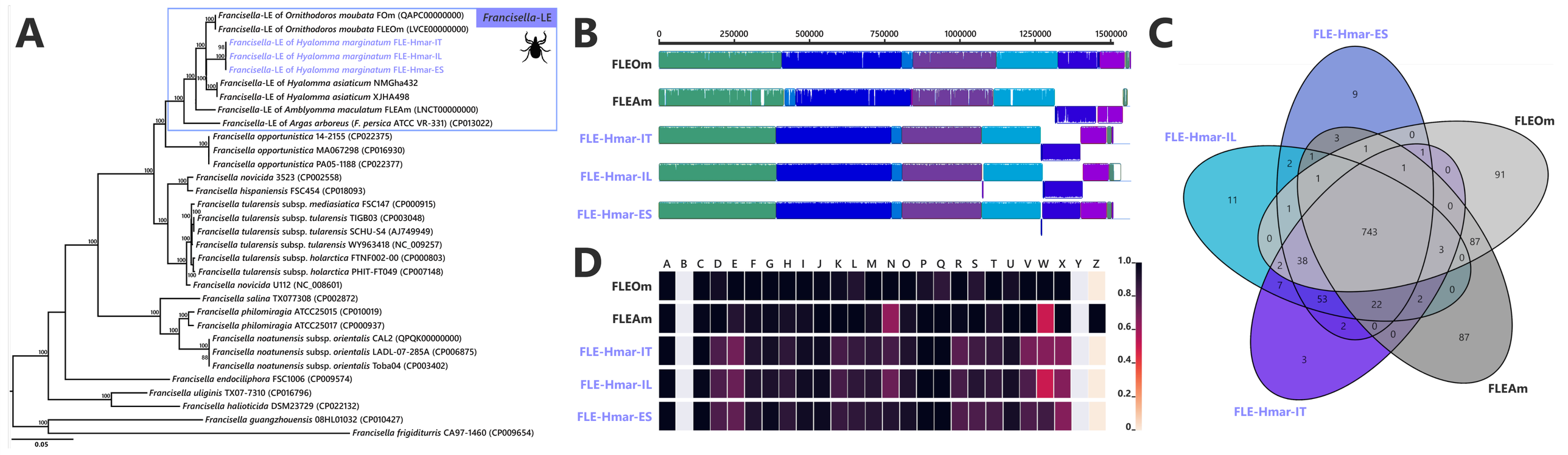
A
Francisella-LE
Francisella-LE of Ornithodoros moubata FOm (QAPC00000000)
Francisella-LE of Ornithodoros moubata FLEOm (LVCE00000000)
Francisella-LE of Hyalomma marginatum FLE-Hmar-IT
Francisella-LE of Hyalomma marginatum FLE-Hmar-IL
Francisella-LE of Hyalomma marginatum FLE-Hmar-ES
Francisella-LE of Hyalomma asiaticum NMGha432
Francisella-LE of Hyalomma asiaticum XJHA498
Francisella-LE of Amblyomma maculatum FLEAm (LNCT00000000)
Francisella-LE of Argas arboreus (F. persica ATCC VR-331) (CP013022)
Francisella opportunistica 14-2155 (CP022375)
Francisella opportunistica MA067298 (CP016930)
Francisella opportunistica PA05-1188 (CP022377)
Francisella novicida 3523 (CP002558)
Francisella hispaniensis FSC454 (CP018093)
Francisella tularensis subsp. mediasiatica FSC147 (CP000915)
Francisella tularensis subsp. tularensis TIGB03 (CP003048)
Francisella tularensis subsp. tularensis SCHU-S4 (AJ749949)
Francisella tularensis subsp. tularensis WY963418 (NC_009257)
Francisella tularensis subsp. holarctica FTNF002-00 (CP000803)
Francisella tularensis subsp. holarctica PHIT-FT049 (CP007148)
Francisella novicida U112 (NC_008601)
Francisella salina TX077308 (CP002872)
Francisella philomiragia ATCC25015 (CP010019)
Francisella philomiragia ATCC25017 (CP000937)
Francisella noatunensis subsp. orientalis CAL2 (QPQK00000000)
Francisella noatunensis subsp. orientalis LADL-07-285A (CP006875)
Francisella noatunensis subsp. orientalis Toba04 (CP003402)
Francisella endociliphora FSC1006 (CP009574)
Francisella uliginis TX07-7310 (CP016796)
Francisella halioticida DSM23729 (CP022132)
Francisella guangzhouensis 08HL01032 (CP010427)
Francisella frigiditurris CA97-1460 (CP009654)
0.05
B
0
250000
500000
750000
1000000
1250000
1500000
FLEOm
FLEAm
FLE-Hmar-IT
FLE-Hmar-IL
FLE-Hmar-ES
C
FLE-Hmar-ES
FLE-Hmar-IL
FLEOm
FLEAm
FLE-Hmar-IT
9
11
91
743
87
38
53
22
87
3
D
A B C D E F G H I J K L M N O P Q R S T U V W X Y Z
FLEOm
FLEAm
FLE-Hmar-IT
FLE-Hmar-IL
FLE-Hmar-ES
1.0
0.8
0.6
0.4
0.2
0

bioRxiv preprint doi: https://doi.org/10.1101/2021.10.12.464044; this version posted October 13, 2021. The copyright holder for this preprint (which was not certified by peer review) is the author/funder, who has granted bioRxiv a license to display the preprint in perpetuity. It is made available under aCC-BY 4.0 International license.

Figure 2. Comparative genomic features of FLE. (A) Whole genome phylogenetic relationship of the three FLE genomes obtained from *H. marginatum* specimens (highlighted), FLE of other tick species, and *Francisella* pathogenic species, including *F. tularensis*. The phylogenetic tree was inferred using maximum likelihood from a concatenated alignment of 436 single-copy orthologous genes (132,718 amino acids; best-fit approximation for the evolutionary model: CPREV+G4+I). The numbers on each node represent the support of 1,000 bootstrap replicates; only bootstrap values >70% are shown. The scale bar is in units of substitution/site. Sequences from newly sequenced FLE genomes are indicated by a blue font.

(B) Whole genome synteny of the three FLE genomes obtained from *H. marginatum* specimens (blue font) and representative FLE (black font). Each contiguously colored locally collinear block (LCB) represents a region without rearrangement of the homologous backbone sequence. LCBs below the center in *Francisella* genomes represent blocks in the reverse orientation. The height of color bars within LCBs corresponds to the average level of similarity (conservation) profile in that region of the genome sequence. Areas that are completely white were not aligned and contain sequence elements specific to a particular genome.

(C) Venn diagram representing orthologs distribution between the three FLE genomes obtained from *H. marginatum* specimens (blue font) and representative FLE (black font).

(D) Clusters of orthologous groups of proteins (COGs) comparisons between the three FLE genomes obtained from *H. marginatum* specimens (blue font) and representative FLE (black font). The color scale indicates the percentage of functional genes per category. Grey color means that genes are not present in a given category. The COG category names (capital letters from A to Z) correspond to the NCBI reference naming system.

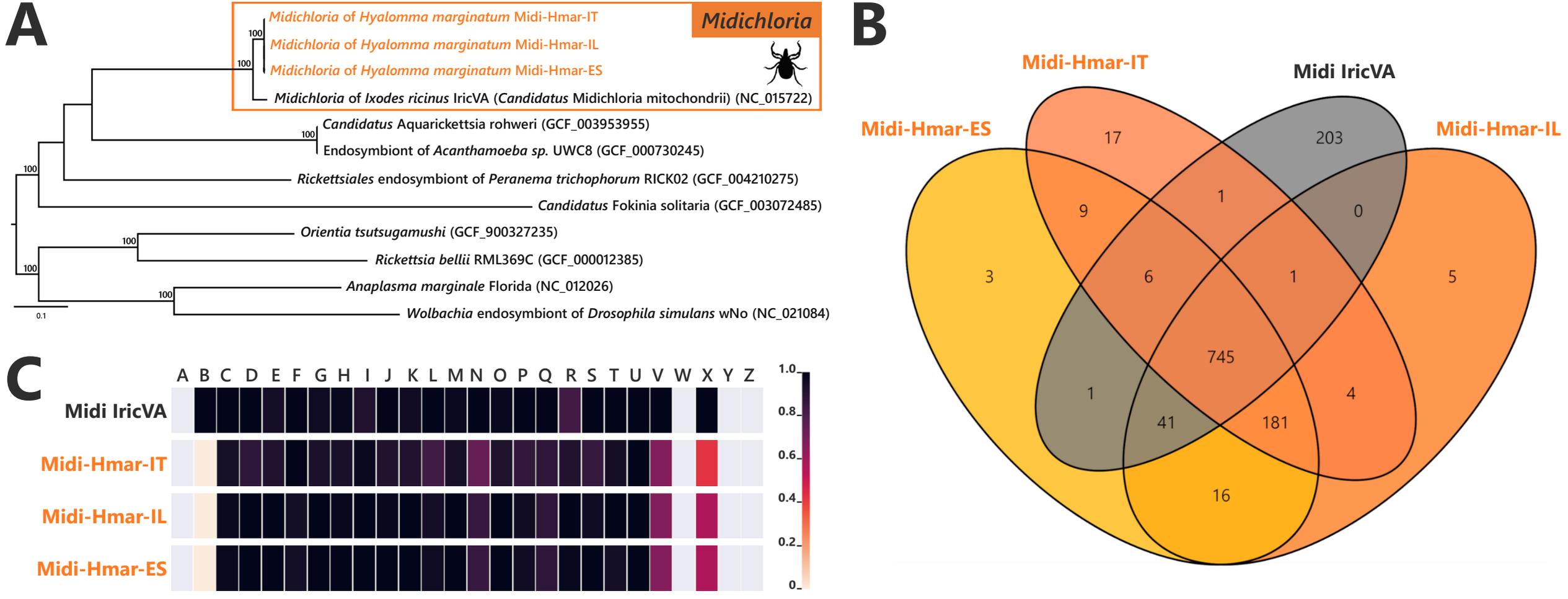
A
Midichloria
Midichloria of Hyalomma marginatum Midi-Hmar-IT
Midichloria of Hyalomma marginatum Midi-Hmar-IL
Midichloria of Hyalomma marginatum Midi-Hmar-ES
Midichloria of Ixodes ricinus IricVA (Candidatus Midichloria mitochondrii) (NC_015722)
Candidatus Aquarickettsia rohweri (GCF_003953955)
Endosymbiont of Acanthamoeba sp. UWC8 (GCF_000730245)
Rickettsiales endosymbiont of Peranema trichophorum RICK02 (GCF_004210275)
Candidatus Fokinia solitaria (GCF_003072485)
Orientia tsutsugamushi (GCF_900327235)
Rickettsia bellii RML369C (GCF_000012385)
Anaplasma marginale Florida (NC_012026)
Wolbachia endosymbiont of Drosophila simulans wNo (NC_021084)
100
0.1
B
Midi-Hmar-IT
Midi IricVA
Midi-Hmar-ES
Midi-Hmar-IL
17
203
9
1
0
3
6
1
5
745
1
4
41
181
16
C
A B C D E F G H I J K L M N O P Q R S T U V W X Y Z
Midi IricVA
Midi-Hmar-IT
Midi-Hmar-IL
Midi-Hmar-ES
1.0
0.8
0.6
0.4
0.2
0

bioRxiv preprint doi: https://doi.org/10.1101/2021.10.12.464044; this version posted October 13, 2021. The copyright holder for this preprint (which was not certified by peer review) is the author/funder, who has granted bioRxiv a license to display the preprint in perpetuity. It is made available under aCC-BY 4.0 International license.

Figure 3. Comparative genomic features of *Midichloria*. (A) Whole genome phylogenetic relationship of the three *Midichloria* genomes obtained from *H. marginatum* specimens (highlighted), *M. mitochondrii*, and other *Rickettsiales* species. The phylogenetic tree was inferred using maximum likelihood from a concatenated alignment of 242 single-copy orthologous genes (49,957 amino acids; best-fit approximation for the evolutionary model: LG+G4+I). The numbers on each node represent the support of 1,000 bootstrap replicates; only bootstrap values >70% are shown. The scale bar is in units of substitution/site. Sequences from newly sequenced *Midichloria* genomes are indicated by an orange font.

(B) Venn diagram representing orthologs distribution between the three *Midichloria* genomes obtained from *H. marginatum* specimens (orange font) and "*Ca*. M. mitochondrii" (black font).

(C) Clusters of Orthologous Groups of proteins (COGs) comparisons between the three *Midichloria* genomes obtained from *H. marginatum* specimens (orange font) and "*Ca*. M. mitochondrii" (black font). The color scale indicates the percentage of functional genes per category. Grey color means that genes are not present in a given category. The COG category names (capital letters from A to Z) correspond to the NCBI reference naming system.

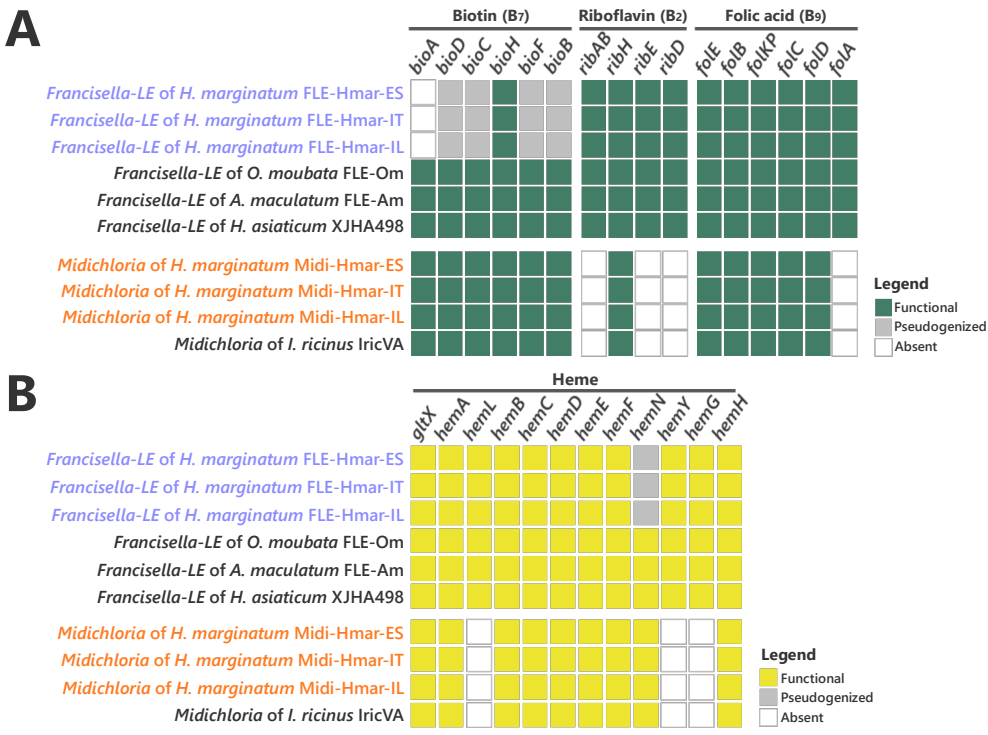
A
Biotin (B7)
Riboflavin (B2)
Folic acid (B9)
bioA
bioD
bioC
bioH
bioF
bioB
ribAB
ribH
ribE
ribD
folE
folB
folKP
folC
folD
folA
Francisella-LE of H. marginatum FLE-Hmar-ES
Francisella-LE of H. marginatum FLE-Hmar-IT
Francisella-LE of H. marginatum FLE-Hmar-IL
Francisella-LE of O. moubata FLE-Om
Francisella-LE of A. maculatum FLE-Am
Francisella-LE of H. asiaticum XJHA498
Midichloria of H. marginatum Midi-Hmar-ES
Midichloria of H. marginatum Midi-Hmar-IT
Midichloria of H. marginatum Midi-Hmar-IL
Midichloria of I. ricinus IricVA
Legend
Functional
Pseudogenized
Absent
B
Heme
gltX
hemA
hemL
hemB
hemC
hemD
hemE
hemF
hemN
hemY
hemG
hemH
Francisella-LE of H. marginatum FLE-Hmar-ES
Francisella-LE of H. marginatum FLE-Hmar-IT
Francisella-LE of H. marginatum FLE-Hmar-IL
Francisella-LE of O. moubata FLE-Om
Francisella-LE of A. maculatum FLE-Am
Francisella-LE of H. asiaticum XJHA498
Midichloria of H. marginatum Midi-Hmar-ES
Midichloria of H. marginatum Midi-Hmar-IT
Midichloria of H. marginatum Midi-Hmar-IL
Midichloria of I. ricinus IricVA
Legend
Functional
Pseudogenized
Absent

bioRxiv preprint doi: https://doi.org/10.1101/2021.10.12.464044; this version posted October 13, 2021. The copyright holder for this preprint (which was not certified by peer review) is the author/funder, who has granted bioRxiv a license to display the preprint in perpetuity. It is made available under aCC-BY 4.0 International license.

Figure 4. Conservation level of biosynthetic pathways involved in the symbiotic interaction between ticks and endosymbionts. (A) Biosynthetic pathways for the three key B vitamins (biotin, folic acid, and riboflavin) required for tick nutrition of FLE, *F. tularensis*, and *Midichloria*. Newly sequenced FLE and *Midichloria* genomes are indicated by a blue and an orange font, respectively. Green squares, functional genes; grey squares, pseudogenes; white squares, missing genes.

(B) Heme biosynthetic pathway of FLE, *F. tularensis*, and *Midichloria*. Newly sequenced FLE and *Midichloria* genomes are indicated by a blue and an orange font, respectively. Yellow squares, functional genes; grey squares, pseudogenes; white squares, missing genes.

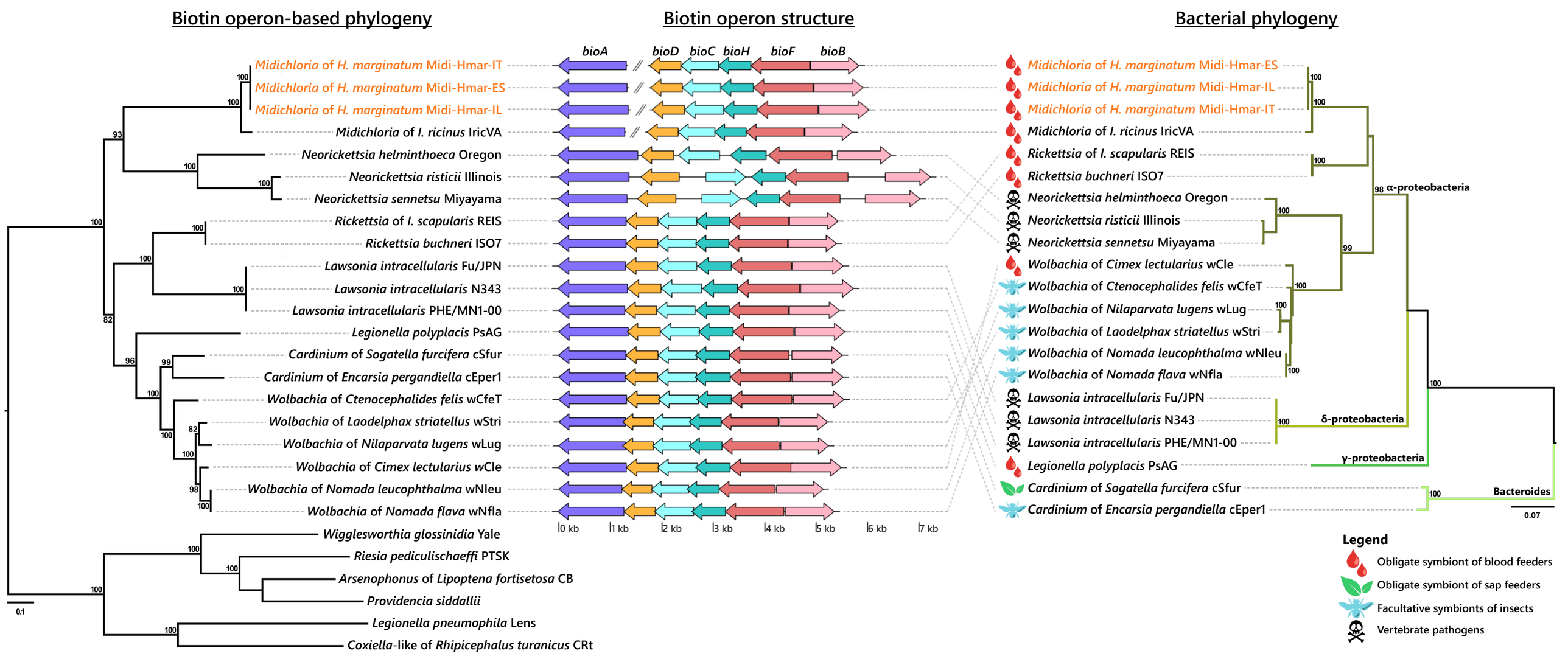
Biotin operon-based phylogeny
Biotin operon structure
Bacterial phylogeny
bioA
bioD
bioC
bioH
bioF
bioB
Midichloria of H. marginatum Midi-Hmar-IT
Midichloria of H. marginatum Midi-Hmar-ES
Midichloria of H. marginatum Midi-Hmar-IL
Midichloria of I. ricinus IricVA
Neorickettsia helminthoeca Oregon
Neorickettsia risticii Illinois
Neorickettsia sennetsu Miyayama
Rickettsia of I. scapularis REIS
Rickettsia buchneri ISO7
Lawsonia intracellularis Fu/JPN
Lawsonia intracellularis N343
Lawsonia intracellularis PHE/MN1-00
Legionella polyplacis PsAG
Cardinium of Sogatella furcifera cSfur
Cardinium of Encarsia pergandiella cEper1
Wolbachia of Ctenocephalides felis wCfeT
Wolbachia of Laodelphax striatellus wStri
Wolbachia of Nilaparvata lugens wLug
Wolbachia of Cimex lectularius wCle
Wolbachia of Nomada leucophthalma wNleu
Wolbachia of Nomada flava wNfla
Wigglesworthia glossinidia Yale
Riesia pediculischaeffi PTSK
Arsenophonus of Lipoptena fortisetosa CB
Providencia siddallii
Legionella pneumophila Lens
Coxiella-like of Rhipicephalus turanicus CRt
0 kb
1 kb
2 kb
3 kb
4 kb
5 kb
6 kb
7 kb
0.1
α-proteobacteria
δ-proteobacteria
γ-proteobacteria
Bacteroides
0.07
Legend
Obligate symbiont of blood feeders
Obligate symbiont of sap feeders
Facultative symbionts of insects
Vertebrate pathogens

bioRxiv preprint doi: https://doi.org/10.1101/2021.10.12.464044; this version posted October 13, 2021. The copyright holder for this preprint (which was not certified by peer review) is the author/funder, who has granted bioRxiv a license to display the preprint in perpetuity. It is made available under aCC-BY 4.0 International license.

Figure 5. Evolutionary relationships (left) and structure (middle) of the streamlined biotin operon, confronted to the bacterial phylogeny (right). The phylogenetic tree of the streamlined biotin operon (left) was inferred using maximum likelihood from a concatenated alignment of the six genes composing the biotin biosynthetic pathway (1,493 amino acids; best-fit approximation for the evolutionary model: CPREV+G4+I). The numbers on each node represent the support of 1,000 bootstrap replicates; only bootstrap values >70% are shown. The scale bar is in units of substitution/site. Sequences from newly sequenced *Midichloria* genomes are indicated by an orange font. Structure of the streamlined biotin operon (middle) is represented by arrows in which each colored arrow corresponds to an intact gene and its direction. A discontinuous line corresponds to genes encoding on two separated contigs. The bacterial phylogenetic tree (right) was inferred using maximum likelihood from an alignment of 16S rDNA sequences (1,362 bp unambiguously aligned; best-fit approximation for the evolutionary model: GTR+G+I). The numbers on each node represent the support of 1,000 bootstrap replicates; only bootstrap values >70% are shown. The scale bar is in units of substitution/site. Sequences from *Midichloria* of *H. marginatum* are indicated by an orange font.

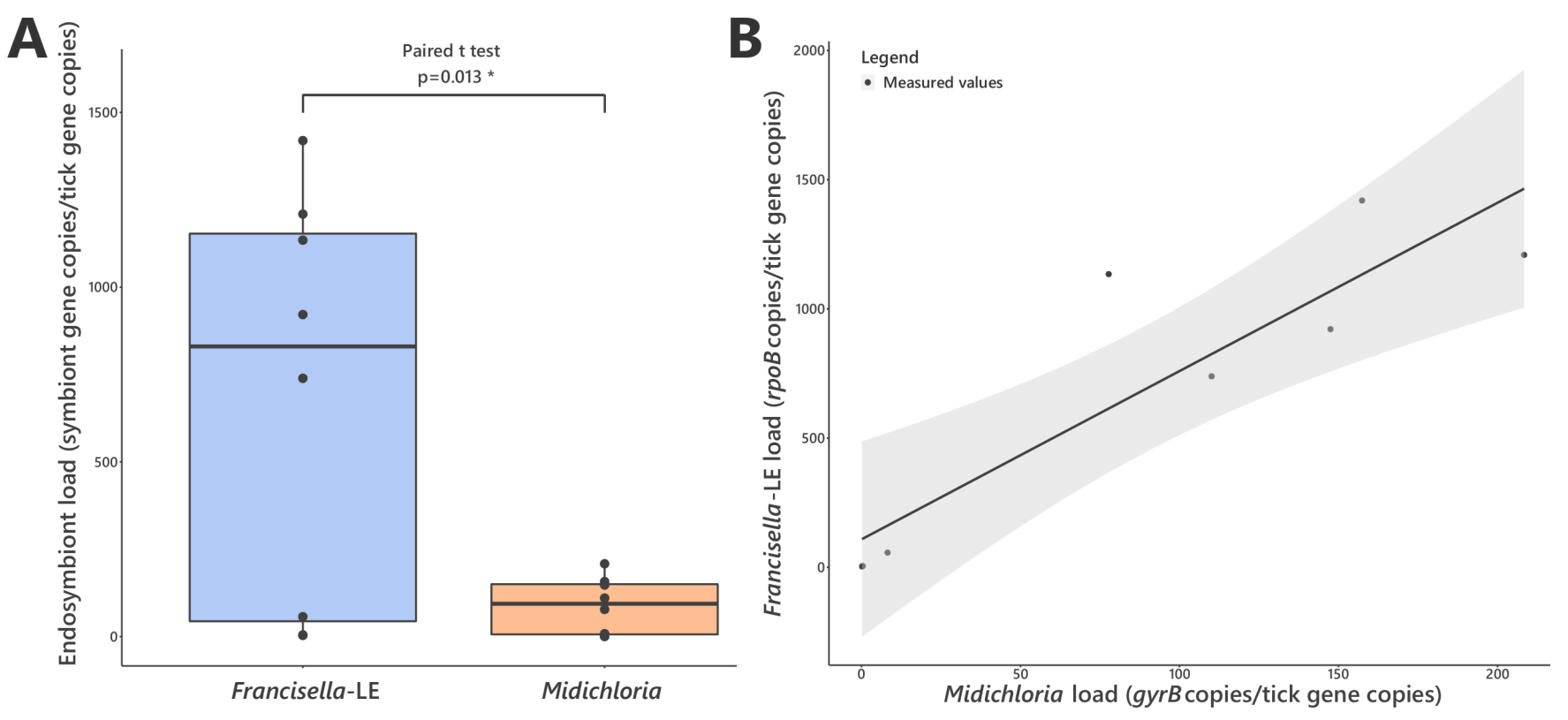
A
Paired t test
p=0.013 *
Endosymbiont load (symbiont gene copies/tick gene copies)
1500
1000
500
0
Francisella-LE
Midichloria
B
Legend
Measured values
Francisella-LE load (rpoB copies/tick gene copies)
2000
1500
1000
500
0
0
50
100
150
200
Midichloria load (gyrB copies/tick gene copies)

bioRxiv preprint doi: https://doi.org/10.1101/2021.10.12.464044; this version posted October 13, 2021. The copyright holder for this preprint (which was not certified by peer review) is the author/funder, who has granted bioRxiv a license to display the preprint in perpetuity. It is made available under aCC-BY 4.0 International license.

Figure 6. FLE and *Midichloria* loads in ovaries of *H. marginatum*. (A) Representation and statistical comparison of FLE and *Midichloria* densities. (B) FLE density as a function of *Midichloria* density in *H. marginatum* ovaries. Grey area represents 95% confidence interval.

bioRxiv preprint doi: https://doi.org/10.1101/2021.10.12.464044; this version posted October 13, 2021. The copyright holder for this preprint (which was not certified by peer review) is the author/funder, who has granted bioRxiv a license to display the preprint in perpetuity. It is made available under aCC-BY 4.0 International license.

SUPPLEMENTARY DATA

A dual endosymbiosis drives nutritional adaptation to hematophagy in the invasive tick *Hyalomma marginatum*

Buysse, Floriano *et al.*

Supplementary table

Table S1. Summary of the assembly information and quality analyses of the newly sequenced genomes of FLE, *Midichloria* and *Rickettsia* bacteria. Only complete genomes are shown and the partial genome of *R. aeaschlimannii* (RAES-Hmar-IS) was not presented.

Specimen details			**Assembling information**								
Genome	Isolate	Origin	Genome size (bp)	Contigs number	N50	L50	Completeness (%)	GC rate (%)	Genes	Pseudogenes	Coding density (%)
Francisella-LE of *Hyalomma marginatum*	FLE-Hmar-ES	Spain	1510123	17	254696	3	0,9905	31,11	937	795	54
Francisella-LE of *Hyalomma marginatum*	FLE-Hmar-IT	Italy	1510130	13	382079	2	0,9905	31,11	934	789	54
Francisella-LE of *Hyalomma marginatum*	FLE-Hmar-IL	Israel	1536710	25	106485	5	0,9905	31,23	961	798	54
Midichloria of *Hyalomma marginatum*	Midi-Hmar-ES	Spain	1168604	179	19210	20	0,981	35,03	1071	192	78
Midichloria of *Hyalomma marginatum*	Midi-Hmar-IT	Italy	1130547	359	10359	30	0,9524	35,23	1032	192	76
Midichloria of *Hyalomma marginatum*	Midi-Hmar-IL	Israel	1144281	123	12627	30	0,981	35,03	1055	190	79
Rickettsia aeschlimannii (of *H. marginatum*)	RAES-Hmar-IT	Italy	1356794	165	67640	4	0,9429	32,32	1122	475	68

Table S2. Summary of the information on the NCBI reference genomes employed for the characterization of the FLE and *Midichloria* genomes.

Specimen details					**Assembling information**			
Genome	Isolate	Origin	Accession number (NCBI/dryad)	Reference	Genome size (bp)	Contigs number	GC rate (%)	Coding density (%)
Francisella-LE of *Ornithodoros moubata*	FLEOm	Lab colony (Czech Republic)	LVCE00000000	Gerhart et al., 2018	1564190	8	31,7	58
Francisella-LE of *Ornithodoros moubata*	FOm	Lab colony (France)	QAPC00000000	Duron et al., 2018	1566493	11	31,7	57
Francisella-LE of *Amblyomma maculatum*	FLEAm	United States of America	LNCT00000000	Gerhart et al., 2018	1556261	7	31,67	57
Francisella-LE of *Argas arboreus*	*F. persica* (ATCC VR-331)	Egypt	CP013022	Larson et al., 2016	1540768	1	31,43	69
Francisella-LE of *Hyalomma asiaticum*	NMGha432	China	doi.org/10.5061/dryad.t76hdr80p	Buysse and Duron, 2021	1550715	38	31,62	58
Francisella-LE of *Hyalomma asiaticum*	XJHA498	China	doi.org/10.5061/dryad.t76hdr80p	Buysse and Duron, 2021	1549389	39	31,6	58
Francisella tularensis (tularemia agent)	SCHU-S4	United States of America	AJ749949	Larsson et al., 2005	1892775	1	32,26	83
Midichloria of *Ixodes ricinus*	IricVA	Italy	CP002130	Sassera et al., 2011	1183732	1	36,55	71

Table S3. Details regarding symbionts used in phylogenetic analyses of B vitamin biosynthetic pathways and streamlined biotin operon of FLE and *Midichloria*.

Specimen details								**Biotin gene origin**	
Class	Order	Family	Genus/Species	Strain	Host species	Accession number	Reference	Horizontal transfer	Ancestral
Gammaproteobacteria	Thiotrichales	Francisellaceae	*Francisella*-like	FLE-Hmar-IL	Hard tick, *Hyalomma marginatum* (Israel)	-	This study		Lost
			Francisella-like	FLE-Hmar-ES	Hard tick, *Hyalomma marginatum* (Spain)	-	This study		Lost
			Francisella-like	FLE-Hmar-IT	Hard tick, *Hyalomma marginatum* (Italy)	-	This study		Lost
			Francisella-like	NMGha432	Hard tick, *Hyalomma asiaticum* (China)	-	Buysse and Duron, 2021		+
			Francisella-like	XJHA498	Hard tick, *Hyalomma asiaticum* (China)	-	Buysse and Duron, 2021		+
			Francisella-like	FLEAm	Hard tick, *Amblyomma maculatum*	LNCT00000000	Gerhart et al., 2018		+
			Francisella-like	FLEOm	Soft tick, *Ornithodoros moubata*	LVCE00000000	Gerhart et al., 2018		+
			Francisella-like	FOm	Soft tick, *Ornithodoros moubata*	QAPC00000000	Duron et al., 2018		+
			Francisella-like	*F. persica*	Soft tick, *Argas arboreus*	CP013022	Suitor and Weiss, 1961		+
	Legionellales	Coxiellaceae	*Coxiella*-like	CRt	Hard tick, *Rhipicephalus turanicus*	CP011126	Gottlieb et al., 2015		+
			Coxiella-like	CRm	Hard tick, *Rhipicephalus microplus*	NSHJ01000000	Guizzo et al., 2017		+
			Coxiella-like	CLEAA	Hard tick, *Amblyomma americanum*	CP007541	Smith et al., 2015		+
			Coxiella-like	CeAS-UFV	Hard tick, *Amblyomma sculptum*	CP033868	Direct submission on GenBank (Vidigal et al.)		+
			Coxiella burnetii	RSA493	-	AE016828	Seshadri et al., 2003		+
		Legionellaceae	*Legionella polyplacis*	PsAG	Louse, *Polyplax serrata*	CP021497	Říhová et al., 2017	+	
			Legionella pneumophila	Lens	-	CR628337	Cazalet et al., 2004		+
	Enterobacterales	Morganellaceae	*Arsenophonus* endosymbiont	CB	Deer ked, *Lipoptena fortisetosa*	CP013920	Direct submission on GenBank (Novakova et al.)		+
			Arsenophonus triatominarum	ATi	Kissing bug, *Triatoma infestans*	LWMI00000000	Direct submission on GenBank (Darby)		+
			Providencia siddallii	officinalis	Leech, *Haementeria officinalis*	CVRF00000000	Direct submission on GenBank (Manzano-Marin)		+
		Erwiniaceae	*Buchnera aphidicola*	LSR1	Aphid, *Acyrthosiphon pisum*	ACFK00000000	Direct submission on GenBank (Shigenobu et al.)		+
			Buchnera aphidicola	-	Aphid, *Myzus persicae*	MJNC00000000	Direct submission on GenBank (Mathers et al.)		+
			Wigglesworthia glossinidia	Yale colony	Tsetse fly, *Glossina morsitans*	CP003315	Rio et al., 2012		+
			Riesia pediculischaeffi	PTSK	Louse, *Pediculus schaeffi*	CP012839	Direct submission on GenBank (Boyd)		+
		Pectobacteriaceae	*Sodalis*-like endosymbiont	IL	Psyllid, *Bactericera trigonica*	RBZS00000000	Ghosh et al., 2020		+
			Sodalis-like endosymbiont	Spu	Cicada, *Philaenus spumarius*	NKXM00000000	Ankrah et al., 2018		+

Alphaproteobacteria	Rickettsiales	Midichloriaceae	*Midichloria*	MID-Hmar-IL	Hard tick, *Hyalomma marginatum* (Israel)	-	This study	+	
			Midichloria	MID-Hmar-ES	Hard tick, *Hyalomma marginatum* (Spain)	-	This study	+	
			Midichloria	MID-Hmar-IT	Hard tick, *Hyalomma marginatum* (Italy)	-	This study	+	
			Cand. Midichloria mitochondrii	IricVA	Hard tick, *Ixodes ricinus*	CP002130	Sassera et al., 2011	+	
		Rickettsiaceae	*Rickettsia buchneri*	ISO7	Hard tick, *Ixodes scapularis*	JFKF00000000	Kurtti et al., 2015	+	
			Rickettsia endosymbiont	REIS	Hard tick, *Ixodes scapularis*	ACLC00000000	Gillespie et al., 2012	+	
			Rickettsia felis	LSU-Lb	Booklouse, *Liposcelis bostrychophila*	JSEL00000000	Gillespie et al., 2014		+
			Rickettsia aeschlimannii	-	-	CCER00000000	Direct submission on GenBank (Urnite platform)		+
		Anaplasmataceae	*Wolbachia*	wNleu	Bee, *Nomada leucophthalma*	LYUV00000000	Direct submission on GenBank (Gerth and Bleidorn)	+	
			Wolbachia	wNfla	Bee, *Nomada flava*	LYUW00000000	Direct submission on GenBank (Gerth and Bleidorn)	+	
			Wolbachia	wCle	Bed bug, *Cimex lectularius*	AP013028	Nikoh et al., 2014	+	
			Wolbachia	wStri	Planthopper, *Laodelphax striatellus*	MUIX00000000	Ju et al., 2020	+	
			Wolbachia	wLug	Planthopper, *Nilaparvata lugens*	MUIY00000000	Ju et al., 2020	+	
			Wolbachia	wCfeT	Flea, *Ctenocephalides felis*	CP051156	Direct submission on GenBank (Driscoll et al.)	+	
			Neorickettsia sennetsu	Miyayama	-	CP000237	Dunning Hotopp et al., 2006	+	
			Neorickettsia risticii	Illinois	-	CP001431	Lin et al., 2009	+	
			Neorickettsia helminthoeca	Oregon	Salmonid fish	CP007481	Direct submission on GenBank (Lin et al.)	+	
			Neorickettsia sp.	179522	-	LNGI00000000	Direct submission on GenBank (Mitreva et al.)	+	
			Ehrlichia ruminantium	Welgevonden	-	CR767821	Collins et al., 2005		+
			Anaplasma marginale	Florida	-	CP001079	Visser et al., 1992		+
Deltaproteobacteria	Desulfovibrionales	Desulfovibrionaceae	*Lawsonia intracellularis*	N343	-	CP004029	Sait et al., 2013	+	
			Lawsonia intracellularis	PHE/MN1-00	-	AM180252	Direct submission on GenBank (Kaur et al.)	+	
			Lawsonia intracellularis	Fu/JPN	-	QNHO00000000	Direct submission on GenBank (Nishikawa et al.)	+	
	Cytophagales	Amoebophilaceae	*Cardinium*	cSfur	Planthopper, *Sogatella furcifera*	CP022339	Direct submission on GenBank (Zeng)	+	
			Cardinium	cEper1	Wasp, *Encarsia pergandiella*	HE983995	Penz et al., 2012	+	
			Cardinium	cBtQ1	Whitefly, *Bemisia tabaci*	CBQZ00000000	Santos-Garcia et al., 2014	+	

Table S4. Illustrative (non-exhaustive) studies investigating the presence of FLE and *Midichloria* symbionts across *Hyalomma* tick species. +: presence; –: absence; ND: not determined.

Specimen details		**Detection details**			
		Symbiont presence			
Tick species	Geographic origin	FLE	*Midichloria*	Detection method	Reference
Hyalomma aegyptium	Israel	+	-	PCR	Azagi et al., 2017
	Anatolia, Mugla Province	+	ND	Metagenomic analysis	Brinkmann et al., 2019
	Qatar, Doha	ND	+	PCR	Barradas et al., 2020
	Bulgaria	+	ND	PCR	Ivanov et al., 2011
H. anatolicum	Turkey	-	-	PCR	Duron et al., 2017
	Turkey	ND	+	PCR & qPCR	Cafiso et al., 2016
	Pakistan, Punjab Province	+	+	Bacterial barcoding	Adegoke et al., 2020
H. asiaticum	China, Xinjiang Province	+	ND	PCR	Wang et al., 2018
	China	+	-	Metagenomic analysis	Buysse and Duron, 2021
H. dromedarii	Israel	+	ND	PCR	Azagi et al., 2017
	Saudi Arabia	+	ND	PCR	Elbir et al., 2020
	Tunisia, Sousse	ND	+	PCR	Selmi et al., 2019
	Tunisia, Kebili	ND	-	PCR	Selmi et al., 2019
	Egypt	+	ND		Ghoneim et al., 2017
	United Arab Emirates, Al-Ain	+	ND	Bacterial barcoding	Perveen et al., 2020
	Palestine, Jericho	+	-	Metagenomic analysis	Ravi et al., 2018
	Saudi Arabia, Al Hofuf	+	-	PCR & bacterial barcoding	Elbir et al., 2019
	Saudi Arabia, Hail Province	+	-	Bacterial barcoding	Alreshidi et al., 2020
H. excavatum	Israel	+	ND	PCR	Azagi et al., 2017
	Tunisia, Kebili	ND	-	PCR	Selmi et al., 2019
	Turkey, Mecitözu	+	+	PCR	Duron et al., 2017
	Turkey	ND	+	PCR & qPCR	Cafiso et al., 2016

	Egypt	ND	+	Reverse line blotting (RLB)	AL-Hosary et al., 2021
H. impeltatum	Tunisia, Gabes	ND	+	PCR	Selmi et al., 2019
	Tunisia, Sousse	ND	+	PCR	Selmi et al., 2019
	Tunisia, Kebili	ND	-	PCR	Selmi et al., 2019
	Tunisia, Kairouan	ND	-	PCR	Selmi et al., 2019
	Tunisia, Tataouine	ND	-	PCR	Selmi et al., 2019
	Zimbabwe	+	-	PCR	Duron et al., 2017
H. lusitanicum	Spain	+	+	Bacterial barcoding	Díaz-Sánchez et al., 2021
	Canaries, Veneguera	+	-	PCR	Duron et al., 2017
	Spain, Madrid	+	ND	PCR	Lopes de Carvalho et al., 2016
	Portugal	-	ND	PCR	Lopes de Carvalho et al., 2016
H. marginatum	Israel	+	ND	PCR & FISH	Azagi et al., 2017
	Anatolia, Mugla Province	+	ND	Illumina HiSeq sequencing	Brinkmann et al., 2019
	France	+	+	PCR	Duron et al., 2017
	Italy, Sicilia	ND	+	PCR	Epis et al., 2008
	Ventotene Island (Mediterranean Sea)	ND	+	PCR	Di Lecce et al., 2018
	Bulgaria	+	ND	PCR	Ivanov et al., 2011
	Spain, Madrid	-	ND	PCR	Lopes de Carvalho et al., 2016
	Portugal	-	ND	PCR	Lopes de Carvalho et al., 2016
H. rufipes	Israel	+	ND	PCR	Azagi et al., 2017
	China, Gansu Province	-	+	High-throughput sequencing of small RNAs	Luo et al., 2017
	Ethiopia, Didessa Valley	+	ND	PCR	Szigeti et al., 2014
H. truncatum	Namibia	+	ND	PCR	Direct submission on GenBank (JF290387)
	Italy, Sicilia	ND	+	PCR	Epis et al., 2008

Table S5. Genes and primers used in this study. Primers were used for qPCR assays conducted for relative quantification of FLE and *Midichloria*.

[1] PCR conditions: primers concentration 150 nM; thermal profile: 95 °C for 3 min, and 40 cycles at 95 °C for 15 sec, 55 °C for 20 sec, 72 °C for 10 sec; [2] PCR conditions: primers concentration 250 nM; thermal profile: 95 °C for 3 min, and 40 cycles at 95 °C for 15 sec, 58 °C for 30 sec; [3] PCR conditions: primers concentration 250 nM; thermal profile: 95 °C for 3 min, and 40 cycles at 95 °C for 15 sec, 58°C for 30 sec.

Gene	Hypothetical product	Primers (5'-3')	Tm (°C)	Fragment size	Reference
Hyalomma marginatum					
cal	Calreticulin	F: TACCTCAAGCTGTTCGACTG R: GCCCTTGTAGTTGAAGATG	53	F/R: 132 bp[1]	This study
FLE					
rpoB	DNA-directed RNA polymerase beta chain	F: TGTACCTATTGCTACGCCAG R: GCTTACCAGTACGACCATC	58	F/R: 122 bp[2]	This study
Midichloria					
gyrB	DNA gyrase B subunit	F: ATTTACATGTCAGGGAGTG R: CTACGAGTTATTGCTGCTC	58	F/R: 155 bp[3]	This study

bioRxiv preprint doi: https://doi.org/10.1101/2021.10.12.464044; this version posted October 13, 2021. The copyright holder for this preprint (which was not certified by peer review) is the author/funder, who has granted bioRxiv a license to display the preprint in perpetuity. It is made available under aCC-BY 4.0 International license.

Supplementary figures

Figure S1. Conservation level of the genes involved in the *Francisella* pathogenicity island (FPI) on FLE of *Hyalomma marginatum* and references genomes. Genomes of FLE of *Hyalomma marginatum* are indicated by a blue font. *Francisella* pathogenic species is indicated by a red font. Red squares, functional genes; grey squares, pseudogenes; white squares, missing genes.

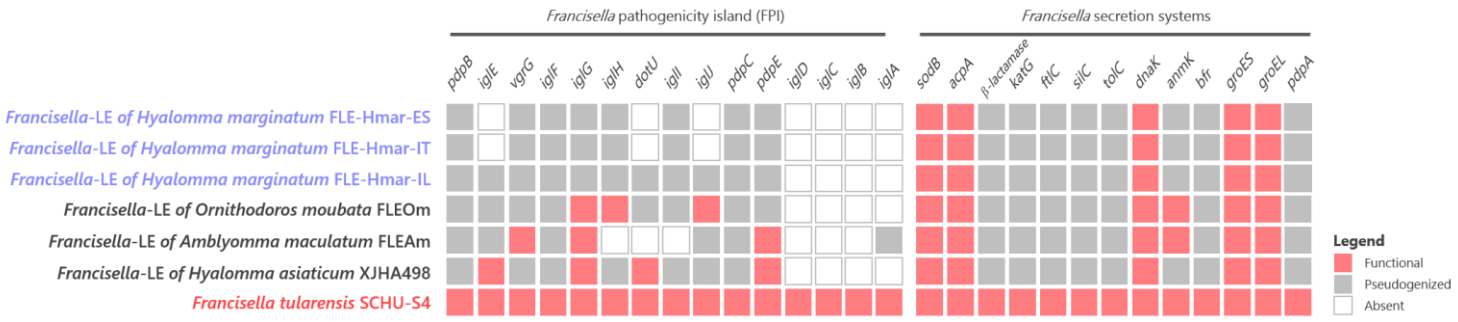

bioRxiv preprint doi: https://doi.org/10.1101/2021.10.12.464044; this version posted October 13, 2021. The copyright holder for this preprint (which was not certified by peer review) is the author/funder, who has granted bioRxiv a license to display the preprint in perpetuity. It is made available under aCC-BY 4.0 International license.

Figure S2. Conservation level of the genes involved in the mismatch repair system (*mutSL*) and the nucleotide excision repair system (*uvrABCD*) on FLE and *Midichloria* of *Hyalomma marginatum* and references genomes. Newly sequenced FLE and *Midichloria* genomes are indicated by a blue and an orange font, respectively. Black squares, functional genes; grey squares, pseudogenes; white squares, missing genes.

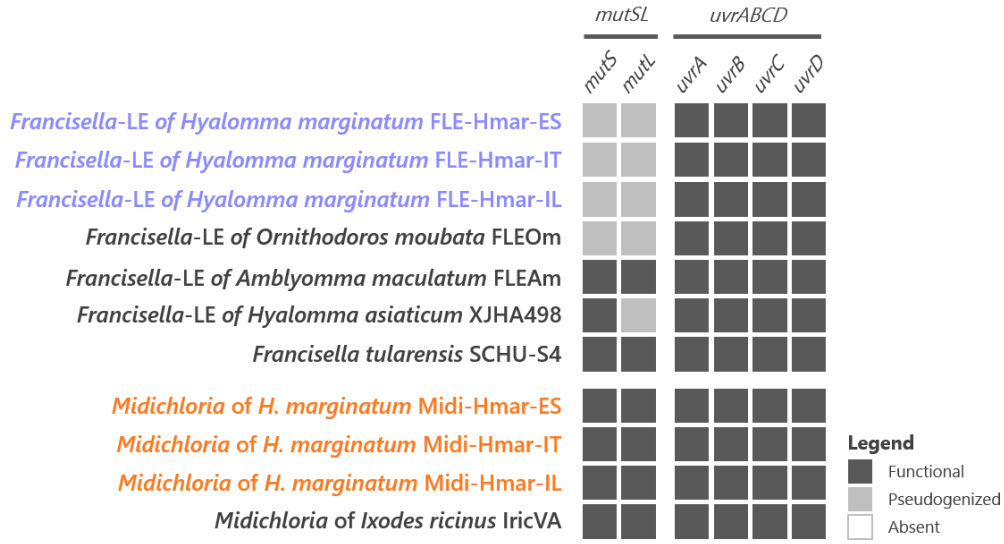

bioRxiv preprint doi: https://doi.org/10.1101/2021.10.12.464044; this version posted October 13, 2021. The copyright holder for this preprint (which was not certified by peer review) is the author/funder, who has granted bioRxiv a license to display the preprint in perpetuity. It is made available under aCC-BY 4.0 International license.

Figure S3. *Rickettsia* phylogenetic tree assessing the affiliation of the *Rickettsia* detected in *Hyalomma marginatum* specimens from Italy and Israel. The phylogenetic tree was inferred using maximum likelihood from a concatenated alignment of 324 single-copy orthologous genes (88,128 amino acids; best-fit approximation for the evolutionary model: JTT+G4+I). The numbers on each node represent the support of 1,000 bootstrap replicates; only bootstrap values >70% are shown. The scale bar is in units of substitution/site. Sequence from the newly sequenced *Rickettsia* genome is indicated by a pink font.

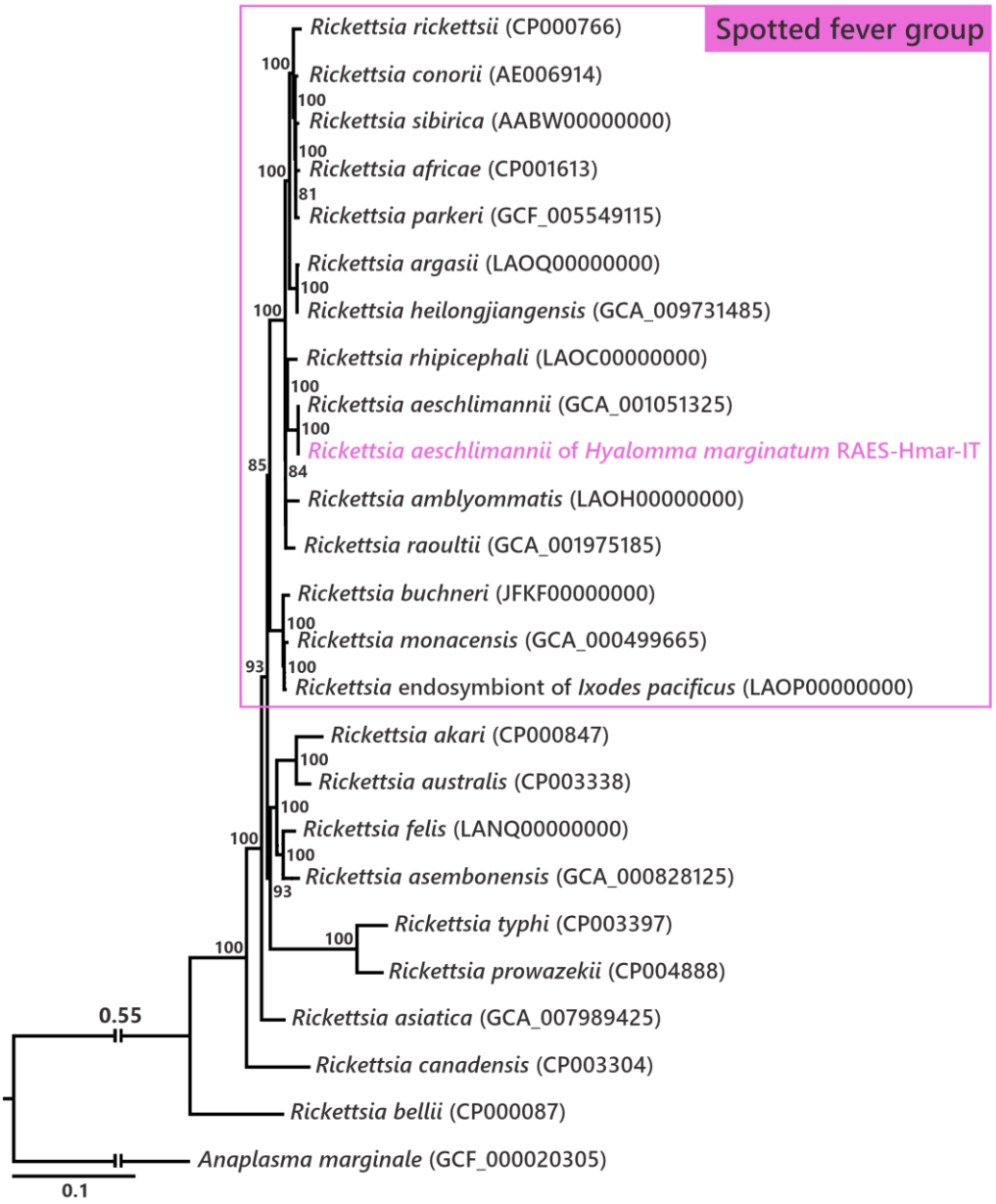

bioRxiv preprint doi: https://doi.org/10.1101/2021.10.12.464044; this version posted October 13, 2021. The copyright holder for this preprint (which was not certified by peer review) is the author/funder, who has granted bioRxiv a license to display the preprint in perpetuity. It is made available under aCC-BY 4.0 International license.

Figure S4. Conservation level of (A) pantothenic acid, nicotinic acid, pyroxidine, and thiamine B vitamins and (B) cofactors biosynthetic pathways of FLE and *Midichloria* symbionts. Newly sequenced FLE and *Midichloria* genomes are indicated by a blue and an orange font, respectively. Green squares, functional genes; grey squares, pseudogenes; white squares, missing genes.

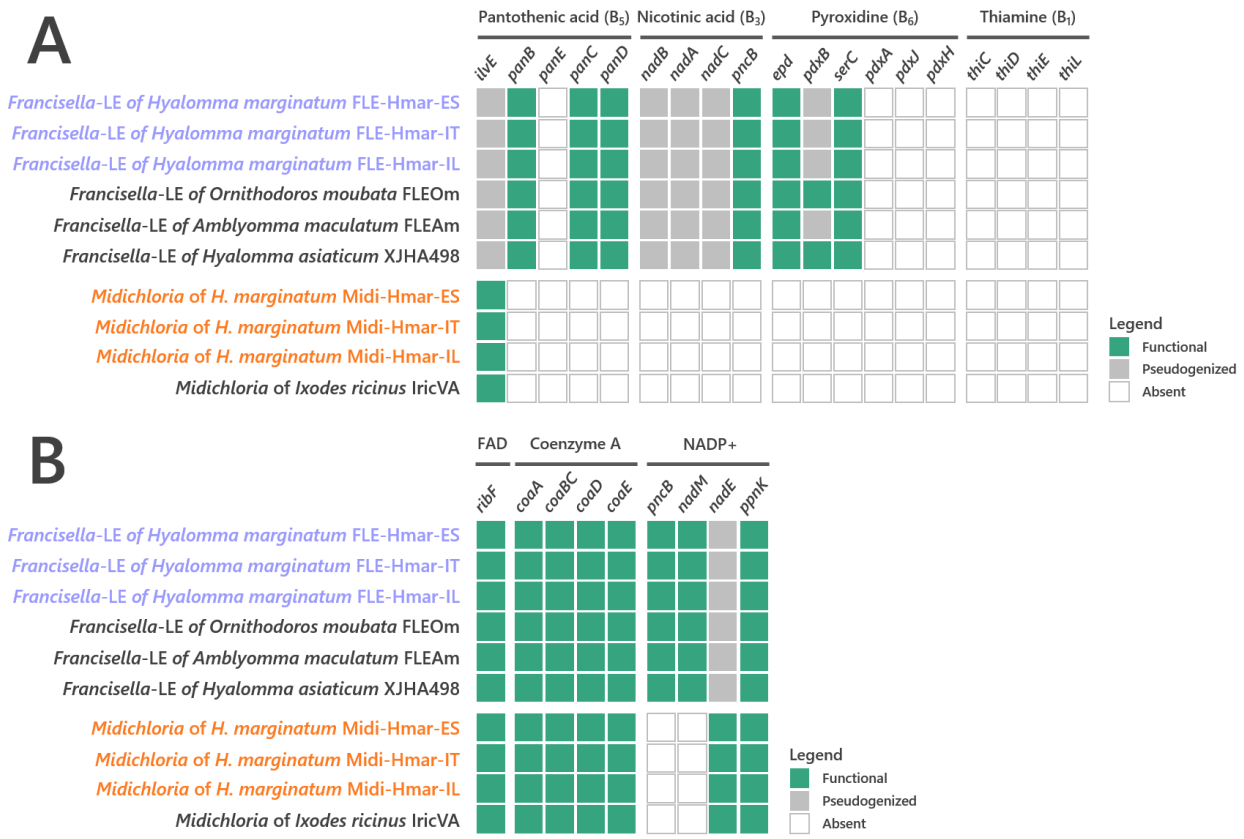

bioRxiv preprint doi: https://doi.org/10.1101/2021.10.12.464044; this version posted October 13, 2021. The copyright holder for this preprint (which was not certified by peer review) is the author/funder, who has granted bioRxiv a license to display the preprint in perpetuity. It is made available under aCC-BY 4.0 International license.

Figure S5. Phylogenetic trees of representative genes of riboflavin and folate biosynthesis pathways of FLE and *Midichloria*. The phylogenetic trees of (A) *ribH* (riboflavin pathway), and (B) *folD* (folate) were inferred using maximum likelihood from amino acid alignments. The numbers on each node represent the support of 1,000 bootstrap replicates; only bootstrap values >70% are shown. The scale bar is in units of substitution/site. *ribH*: 129 amino acids unambiguously aligned, best-fit approximation for the evolutionary model LG+G4; *folD*: 273 amino acids unambiguously aligned, best-fit approximation for the evolutionary model CPREV+G4+I. Newly sequenced FLE and *Midichloria* sequences are indicated by a blue and an orange font, respectively, while sequences from other FLE and *Midichloria* are highlighted in blue and orange, respectively.

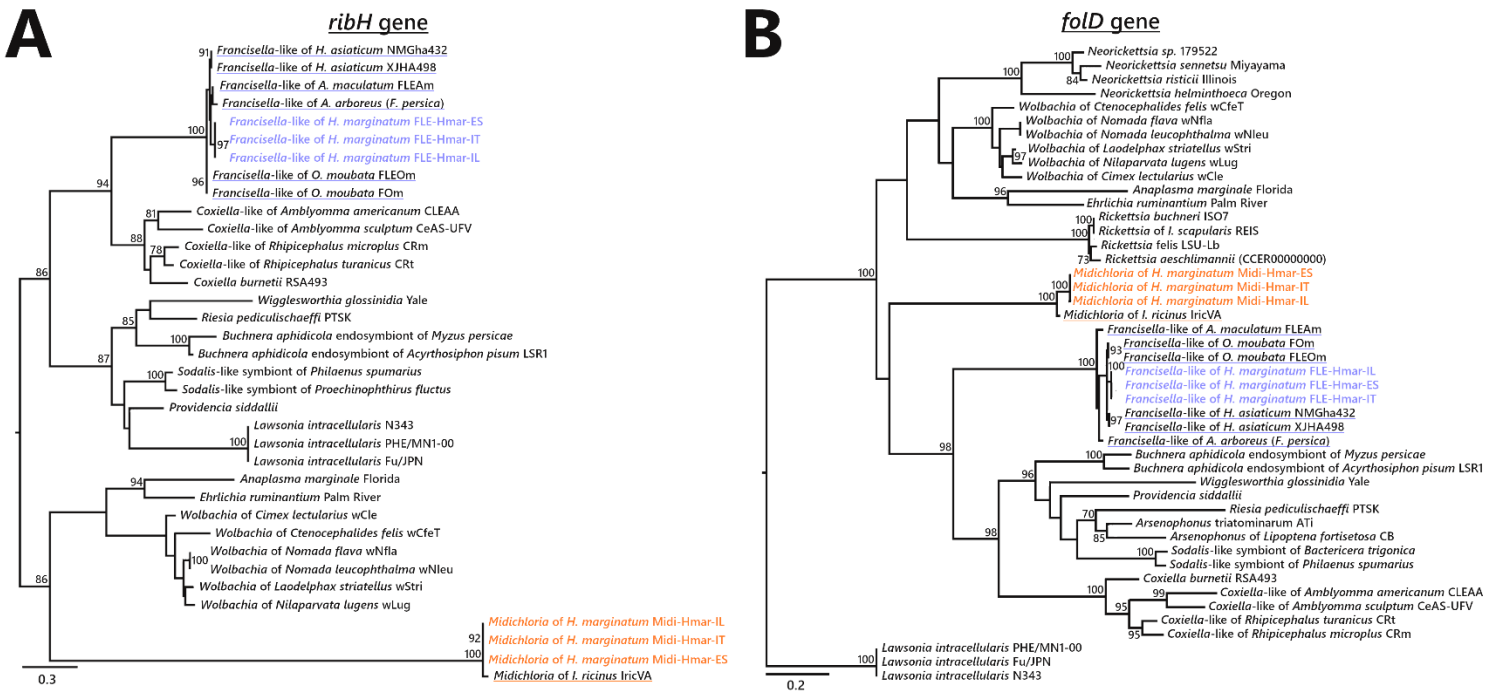

bioRxiv preprint doi: https://doi.org/10.1101/2021.10.12.464044; this version posted October 13, 2021. The copyright holder for this preprint (which was not certified by peer review) is the author/funder, who has granted bioRxiv a license to display the preprint in perpetuity. It is made available under aCC-BY 4.0 International license.

Figure S6. Phylogenetic relationship of the *Hyalomma* species used in our study. The phylogenetic tree was inferred using maximum likelihood from an alignment of the cytochrome c oxidase I (*cox1*) gene sequences (546 bp unambiguously aligned, best-fit approximation for the evolutionary model: HKY+G+I). The numbers on each node represent the support of 1,000 bootstrap replicates; only bootstrap values >80% are shown. The scale bar is in units of substitution/site.

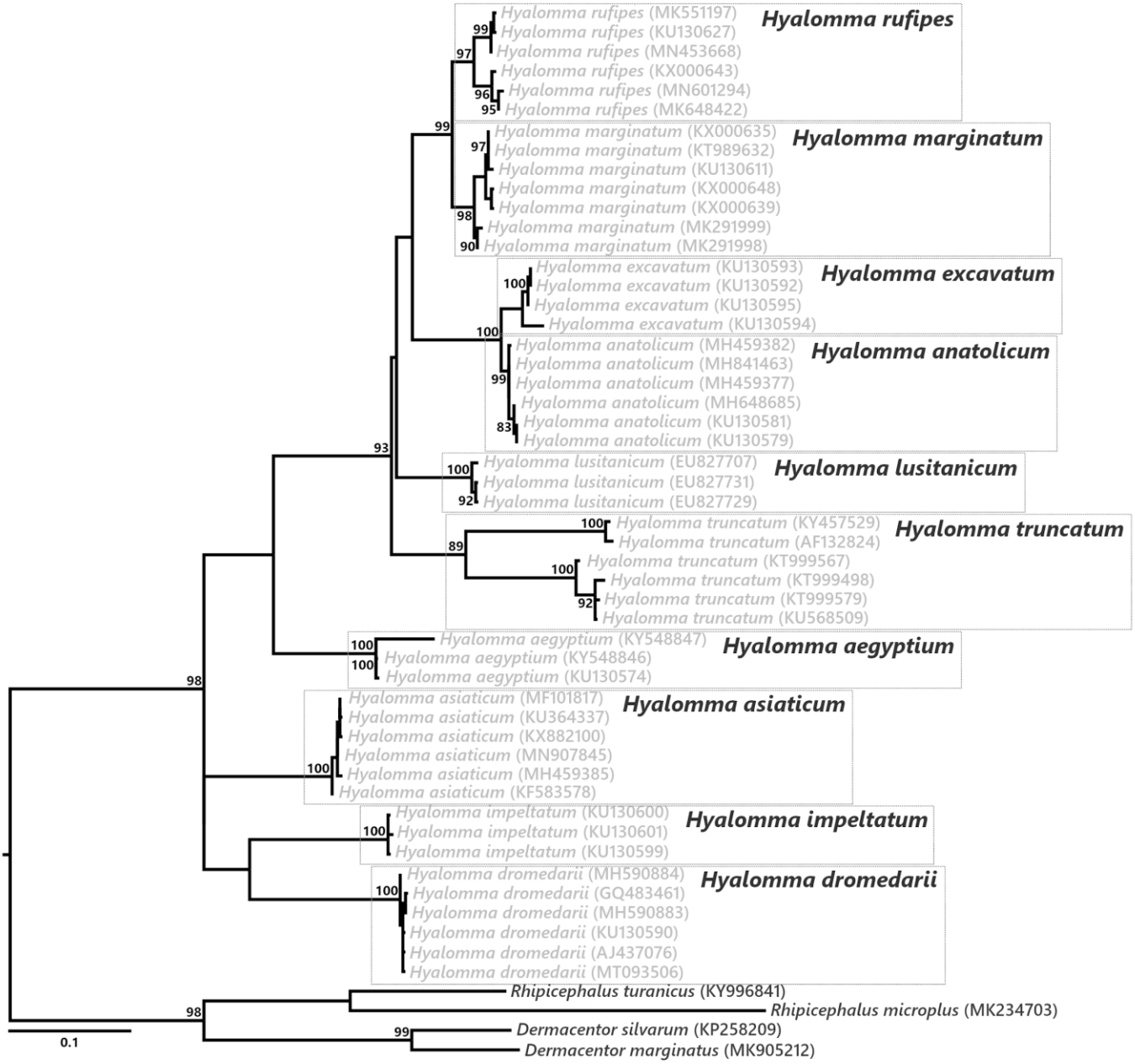

bioRxiv preprint doi: https://doi.org/10.1101/2021.10.12.464044; this version posted October 13, 2021. The copyright holder for this preprint (which was not certified by peer review) is the author/funder, who has granted bioRxiv a license to display the preprint in perpetuity. It is made available under aCC-BY 4.0 International license.

Figure S7. Presence of FLE and *Midichloria* within the *Hyalomma* genus. The *Hyalomma* cladogram was adapted from *cox1* phylogeny showed at Figure S6. The numbers on each node represent the support of 1,000 bootstrap replicates; only bootstrap values >80% are shown. The scale bar is in units of substitution/site. Blue and orange plain circles indicate the presence of FLE and *Midichloria*, respectively, as detailed in Table S4. Blank circle represents an absence of symbiont.

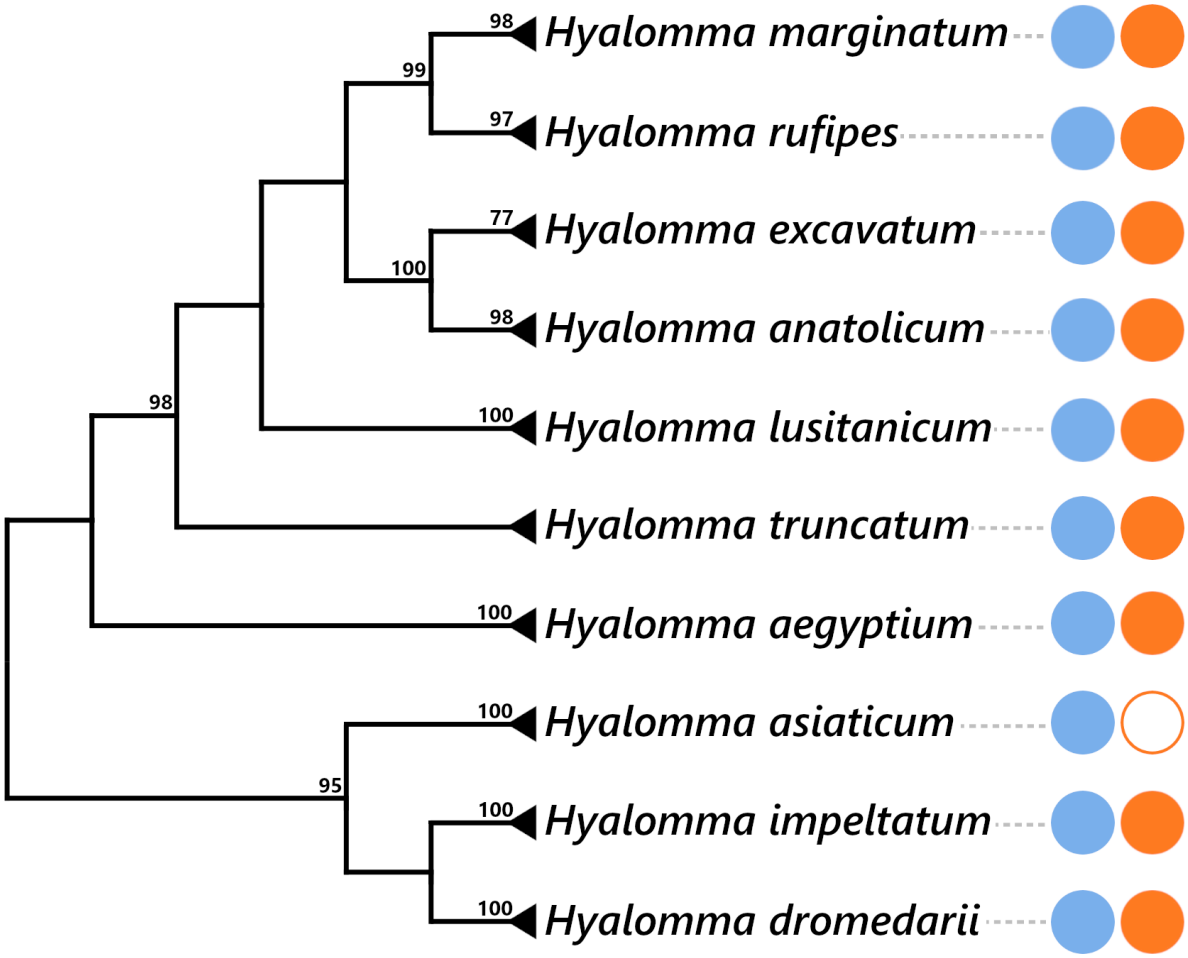

bioRxiv preprint doi: https://doi.org/10.1101/2021.10.12.464044; this version posted October 13, 2021. The copyright holder for this preprint (which was not certified by peer review) is the author/funder, who has granted bioRxiv a license to display the preprint in perpetuity. It is made available under aCC-BY 4.0 International license.

Supplementary references

Adegoke A, Kumar D, Bobo C, Rashid MI, Durrani AZ, Sajid MS, Karim S. 2020. Tick-borne pathogens shape the native microbiome within tick vectors. *Microorganisms* **8**:1–16. doi:10.3390/microorganisms8091299

AL-Hosary A, Răileanu C, Tauchmann O, Fischer S, Nijhof AM, Silaghi C. 2021. Tick species identification and molecular detection of tick-borne pathogens in blood and ticks collected from cattle in Egypt. *Ticks Tick Borne Dis* **12**. doi:10.1016/j.ttbdis.2021.101676

Alreshidi MM, Veettil VN, Noumi E, Del Campo R, Snoussi M. 2020. Description of microbial diversity associated with ticks *Hyalomma dromedarii* (Acari: Ixodidae) isolated from camels in Hail region (Saudi Arabia) using massive sequencing of 16S rDNA. *Bioinformation* **16**:602–610. doi:10.6026/97320630016602

Ankrah NYD, Chouaia B, Douglas E. 2018. The cost of metabolic interactions in symbioses between insects and bacteria with reduced genomes. *MBio* **9**:1–15. doi: 10.1128/mBio.01433-18

Azagi T, Klement E, Perlman G, Lustig Y, Mumcuoglu KY, Apanaskevich DA, Gottlieb Y. 2017. *Francisella*-like endosymbionts and *Rickettsia* species in local and imported *Hyalomma* ticks. *Appl Environ Microbiol* **83**:1–14. doi:10.1128/AEM.01302-17

Barradas PF, Lima C, Cardoso L, Amorim I, Gärtner F, Mesquita JR. 2020. Molecular evidence of *Hemolivia mauritanica, Ehrlichia spp.* and the endosymbiont *Candidatus* Midichloria mitochondrii in *Hyalomma aegyptium* infesting *Testudo graeca* tortoises from Doha, Qatar. *animals*. doi:10.3390/ani11010030

Brinkmann A, Hekimoğlu O, Dinçer E, Hagedorn P, Nitsche A, Ergünay K. 2019. A cross-sectional screening by next-generation sequencing reveals *Rickettsia*, *Coxiella*, *Francisella*, *Borrelia*, *Babesia*, *Theileria* and *Hemolivia* species in ticks from Anatolia.

bioRxiv preprint doi: https://doi.org/10.1101/2021.10.12.464044; this version posted October 13, 2021. The copyright holder for this preprint (which was not certified by peer review) is the author/funder, who has granted bioRxiv a license to display the preprint in perpetuity. It is made available under aCC-BY 4.0 International license.

Parasites and Vectors **12**:1–13. doi:10.1186/s13071-018-3277-7

Buysse M, Duron O. 2021. Evidence that microbes identified as tick-borne pathogens are nutritional endosymbionts. *Cell*. doi: 10.1016/j.cell.2021.03.053

Cafiso A, Bazzocchi C, De Marco L, Opara MN, Sassera D, Plantard O. 2016. Molecular screening for *Midichloria* in hard and soft ticks reveals variable prevalence levels and bacterial loads in different tick species. *Ticks Tick Borne Dis* **7**:1186–1192. doi:10.1016/j.ttbdis.2016.07.017

Cazalet C, Rusniok C, Brüggemann H, Zidane N, Magnier A, Ma L, Tichit M, Jarraud S, Bouchier C, Vandenesch F, Kunst F, Etienne J, Glaser P, Buchrieser C. 2004. Evidence in the *Legionella pneumophila* genome for exploitation of host cell functions and high genome plasticity. *Nat Genet* **36**:1165–1173. doi:10.1038/ng1447

Collins NE, Liebenberg J, De Villiers EP, Brayton KA, Louw E, Pretorius A, Faber FE, Van Heerden H, Josemans A, Van Kleef M, Steyn HC, Van Strijp MF, Zweygarth E, Jongejan F, Maillard JC, Berthier D, Botha M, Joubert F, Corton CH, Thomson NR, Allsopp MT, Allsopp BA. 2005. The genome of the heartwater agent *Ehrlichia ruminantium* contains multiple tandem repeats of actively variable copy number. *Proc Natl Acad Sci U S A* **102**:838–843. doi:10.1073/pnas.0406633102

Di Lecce I, Bazzocchi C, Cecere JG, Epis S, Sassera D, Villani BM, Bazzi G, Negri A, Saino N, Spina F, Bandi C, Rubolini D. 2018. Patterns of *Midichloria* infection in avian-borne African ticks and their trans-Saharan migratory hosts. *Parasites and Vectors* **11**:1–11. doi:10.1186/s13071-018-2669-z

Díaz-Sánchez S, Fernández AM, Habela MA, Calero-Bernal R, de Mera IGF, de la Fuente J. 2021. Microbial community of *Hyalomma lusitanicum* is dominated by *Francisella*-like endosymbiont. *Ticks Tick Borne Dis* **12**. doi:10.1016/j.ttbdis.2020.101624

Dunning Hotopp JC, Lin M, Madupu R, Crabtree J, Angiuoli S V., Eisen J, Seshadri R, Ren Q, Wu M, Utterback TR, Smith S, Lewis M, Khouri H, Zhang C, Niu H, Lin Q, Ohashi

bioRxiv preprint doi: https://doi.org/10.1101/2021.10.12.464044; this version posted October 13, 2021. The copyright holder for this preprint (which was not certified by peer review) is the author/funder, who has granted bioRxiv a license to display the preprint in perpetuity. It is made available under aCC-BY 4.0 International license.

N, Zhi N, Nelson W, Brinkac LM, Dodson RJ, Rosovitz MJ, Sundaram J, Daugherty SC, Davidsen T, Durkin AS, Gwinn M, Haft DH, Selengut JD, Sullivan SA, Zafar N, Zhou L, Benahmed F, Forberger H, Halpin R, Mulligan S, Robinson J, White O, Rikihisa Y, Tettelin H. 2006. Comparative genomics of emerging human ehrlichiosis agents. *PLoS Genet* **2**:208–223. doi:10.1371/journal.pgen.0020021

Duron O, Binetruy F, Noel V, Cremaschi J, McCoy K, Arnathau C, Plantard O, Goolsby J, Perez De Leon AA, Heylen DJA, Raoul Van Oosten A, Gottlieb Y, Baneth G, Guglielmone AA, Estrada-Pena A, Opara MN, Zenner L, Vavre F, Chevillon C. 2017. Evolutionary changes in symbiont community structure in ticks. *Mol Ecol* **26**:2905–2921. doi:10.1111/mec.14094

Duron O, Morel O, Noël V, Buysse M, Binetruy F, Lancelot R, Loire E, Ménard C, Bouchez O, Vavre F, Vial L. 2018. Tick-bacteria mutualism depends on B vitamin synthesis pathways. *Curr Biol* **28**:1–7. doi:10.1016/j.cub.2018.04.038

Elbir H, Almathen F, Alhumam NA. 2019. A glimpse of the bacteriome of *Hyalomma dromedarii* ticks infesting camels reveals human Helicobacter pylori pathogen. *J Infect Dev Ctries* **13**:1001–1012. doi:10.3855/JIDC.11604

Elbir H, Almathen F, Elnahas A. 2020. Low genetic diversity among *Francisella*-like endosymbionts within different genotypes of *Hyalomma dromedarii* ticks infesting camels in Saudi Arabia. *Vet World* **13**:1462–1472. doi:10.14202/vetworld.2020.1462-1472

Epis S, Sassera D, Beninati T, Lo N, Beati L, Piesman J, Rinaldi L, McCoy KD, Torina A, Sacchi L, Clementi E, Genchi M, Magnino S, Bandi C. 2008. *Midichloria mitochondrii* is widespread in hard ticks (Ixodidae) and resides in the mitochondria of phylogenetically diverse species. *Parasitology* **135**:485–494. doi:10.1017/S0031182007004052

Gerhart JG, Auguste Dutcher H, Brenner AE, Moses AS, Grubhoffer L, Raghavan R. 2018.

bioRxiv preprint doi: https://doi.org/10.1101/2021.10.12.464044; this version posted October 13, 2021. The copyright holder for this preprint (which was not certified by peer review) is the author/funder, who has granted bioRxiv a license to display the preprint in perpetuity. It is made available under aCC-BY 4.0 International license.

Multiple acquisitions of pathogen-derived *Francisella* endosymbionts in soft ticks. *Genome Biol Evol* **10**:607–615. doi:10.1093/gbe/evy021

Ghoneim NH, Abdel-Moein KA, Zaher HM. 2017. Molecular detection of *Francisella spp*. among ticks attached to camels in Egypt. *Vector-Borne Zoonotic Dis* **17**:384–387. doi:10.1089/vbz.2016.2100

Ghosh S, Sela N, Kontsedalov S, Lebedev G, Haines LR, Ghanim M. 2020. An intranuclear *Sodalis*-like symbiont and *Spiroplasma* coinfect the carrot psyllid, *Bactericera trigonic*a (Hemiptera, Psylloidea). *microorganisms* **8**. doi: 10.3390/microorganisms8050692

Gillespie JJ, Drisco TP, Verhoeve VI, Utsuki T, Husseneder C, Chouljenko VN, Azad AF, MacAluso KR. 2014. Genomic diversification in strains of *Rickettsia felis* isolated from different arthropods. *Genome Biol Evol* **7**:35–56. doi:10.1093/gbe/evu262

Gillespie JJ, Joardar V, Williams KP, Driscoll T, Hostetler JB, Nordberg E, Shukla M, Walenz B, Hill CA, Nene VM, Azad AF, Sobral BW, Caler E. 2012. A *Rickettsia* genome overrun by mobile genetic elements provides insight into the acquisition of genes characteristic of an obligate intracellular lifestyle. *J Bacteriol* **194**:376–394. doi:10.1128/JB.06244-11

Gottlieb Y, Lalzar I, Klasson L. 2015. Distinctive genome reduction rates revealed by genomic analyses of two *Coxiella*-like endosymbionts in ticks. *Genome Biol Evol* **7**:1779–1796. doi:10.1093/gbe/evv108

Guizzo MG, Parizi LF, Nunes RD, Schama R, Albano RM, Tirloni L, Oldiges DP, Vieira RP, Oliveira WHC, Leite MDS, Gonzales SA, Farber M, Martins O, Vaz IDS, Oliveira PL. 2017. A *Coxiella* mutualist symbiont is essential to the development of *Rhipicephalus microplus*. *Sci Rep* **7**:1–10. doi:10.1038/s41598-017-17309-x

Ivanov IN, Mitkova N, Reye AL, Hübschen JM, Vatcheva-Dobrevska RS, Dobreva EG, Kantardjiev T V., Muller CP. 2011. Detection of new *Francisella*-like tick endosymbionts in *Hyalomma spp.* and *Rhipicephalus spp.* (Acari: Ixodidae) from

bioRxiv preprint doi: https://doi.org/10.1101/2021.10.12.464044; this version posted October 13, 2021. The copyright holder for this preprint (which was not certified by peer review) is the author/funder, who has granted bioRxiv a license to display the preprint in perpetuity. It is made available under aCC-BY 4.0 International license.

Bulgaria. *Appl Environ Microbiol* **77**:5562–5565. doi:10.1128/AEM.02934-10

Ju JF, Bing XL, Zhao DS, Guo Y, Xi Z, Hoffmann AA, Zhang KJ, Huang HJ, Gong JT, Zhang X, Hong XY. 2020. *Wolbachia* supplement biotin and riboflavin to enhance reproduction in planthoppers. *ISME J* **14**:676–687. doi:10.1038/s41396-019-0559-9

Kurtti TJ, Felsheim RF, Burkhardt NY, Oliver JD, Heu CC, Munderloh UG. 2015. *Rickettsia buchneri* sp. nov., a rickettsial endosymbiont of the blacklegged tick *Ixodes scapularis*. *Int J Syst Evol Microbiol* **65**:965–970. doi:10.1099/ijs.0.000047

Larsson P, Oyston PCF, Chain P, Chu MC, Duffield M, Fuxelius HH, Garcia E, Hälltorp G, Johansson D, Isherwood KE, Karp PD, Larsson E, Liu Y, Michell S, Prior J, Prior R, Malfatti S, Sjöstedt A, Svensson K, Thompson N, Vergez L, Wagg JK, Wren BW, Lindler LE, Andersson SGE, Forsman M, Titball RW. 2005. The complete genome sequence of *Francisella tularensis*, the causative agent of tularemia. *Nat Genet* **37**:153–159. doi:10.1038/ng1499

Lin M, Zhang C, Gibson K, Rikihisa Y. 2009. Analysis of complete genome sequence of *Neorickettsia risticii*: Causative agent of Potomac horse fever. *Nucleic Acids Res* **37**:6076–6091. doi:10.1093/nar/gkp642

Lopes de Carvalho I, Toledo A, Carvalho CL, Barandika JF, Respicio-Kingry LB, Garcia-Amil C, García-Pérez AL, Olmeda AS, Zé-Zé L, Petersen JM, Anda P, Núncio MS, Escudero R. 2016. *Francisella* species in ticks and animals, Iberian Peninsula. *Ticks Tick Borne Dis* **7**:159–165. doi:10.1016/j.ttbdis.2015.10.009

Luo J, Liu MX, Ren QY, Chen Z, Tian ZC, Hao JW, Wu F, Liu XC, Luo JX, Yin H, Wang H, Liu GY. 2017. Micropathogen community analysis in *Hyalomma rufipes* via high-throughput sequencing of small RNAs. *Front Cell Infect Microbiol* **7**:1–12. doi:10.3389/fcimb.2017.00374

Nikoh N, Hosokawa T, Moriyama M, Oshima K, Hattori M, Fukatsu T. 2014. Evolutionary origin of insect-*Wolbachia* nutritional mutualism. *Proc Natl Acad Sci U S A* **111**:10257–

bioRxiv preprint doi: https://doi.org/10.1101/2021.10.12.464044; this version posted October 13, 2021. The copyright holder for this preprint (which was not certified by peer review) is the author/funder, who has granted bioRxiv a license to display the preprint in perpetuity. It is made available under aCC-BY 4.0 International license.

10262. doi:10.1073/pnas.1409284111

Penz T, Schmitz-Esser S, Kelly SE, Cass BN, Müller A, Woyke T, Malfatti SA, Hunter MS, Horn M. 2012. Comparative genomics suggests an independent origin of cytoplasmic incompatibility in *Cardinium hertigii*. *PLoS Genet* **8**. doi:10.1371/journal.pgen.1003012

Perveen N, Muzaffar S Bin, Vijayan R, Al-Deeb MA. 2020. Microbial communities associated with the camel tick, Hyalomma dromedarii: 16S rRNA gene-based analysis. *Sci Rep* **10**:1–11. doi:10.1038/s41598-020-74116-7

Ravi A, Ereqat S, Al-Jawabreh A, Abdeen Z, Shamma OA, Hall H, Pallen MJ, Nasereddin A. 2018. Metagenomic profiling of ticks: Identification of novel rickettsial genomes and detection of tick borne canine parvovirus. *bioRxiv* 1–19. doi:10.1101/407510

Říhová J, Novaková E, Husník F, Hypša V. 2017. *Legionella* becoming a mutualist: Adaptive processes shaping the genome of symbiont in the louse *Polyplax serrata*. *Genome Biol Evol* **9**:2946–2957. doi:10.1093/gbe/evx217

Rio RVM, Symula RE, Wang J, Lohs C, Wu Y neng, Snyder AK, Bjornson RD, Oshima K, Biehl BS, Perna NT, Hattori M, Aksoy S. 2012. Insight into the transmission biology and species-specific functional capabilities of Tsetse (Diptera: Glossinidae) obligate symbiont *Wigglesworthia*. *MBio* **3**:1–13. doi:10.1128/mBio.00240-11

Sait M, Aitchison K, Wheelhouse N, Wilson K, Lainson FA, Longbottom D, Smith DGE. 2013. Genome sequence of *Lawsonia intracellularis* strain N343, isolated from a sow with hemorrhagic proliferative enteropathy. *Genome Announc* **1**:1–2. doi:10.1128/genomeA.00027-13

Santos-Garcia D, Rollat-Farnier PA, Beitia F, Zchori-Fein E, Vavre F, Mouton L, Moya A, Latorre A, Silva FJ. 2014. The genome of *Cardinium* cBtQ1 provides insights into genome reduction, symbiont motility, and its settlement in *Bemisia tabaci*. *Genome Biol Evol* **6**:1013–1030. doi:10.1093/gbe/evu077

Sassera D, Lo N, Epis S, D'Auria G, Montagna M, Comandatore F, Horner D, Peretó J,

bioRxiv preprint doi: https://doi.org/10.1101/2021.10.12.464044; this version posted October 13, 2021. The copyright holder for this preprint (which was not certified by peer review) is the author/funder, who has granted bioRxiv a license to display the preprint in perpetuity. It is made available under aCC-BY 4.0 International license.

Luciano AM, Franciosi F, Ferri E, Crotti E, Bazzocchi C, Daffonchio D, Sacchi L, Moya A, Latorre A, Bandi C. 2011. Phylogenomic evidence for the presence of a flagellum and cbb3 oxidase in the free-living mitochondrial ancestor. *Mol Biol Evol* **28**:3285–3296. doi:10.1093/molbev/msr159

Selmi R, Ben Said M, Mamlouk A, Ben Yahia H, Messadi L. 2019. Molecular detection and genetic characterization of the potentially pathogenic *Coxiella burnetii* and the endosymbiotic *Candidatus* Midichloria mitochondrii in ticks infesting camels (*Camelus dromedarius*) from Tunisia. *Microb Pathog* **136**:103655. doi:10.1016/j.micpath.2019.103655

Seshadri R, Paulsen IT, Eisen JA, Read TD, Nelson KE, Nelson WC, Ward NL, Tettelin H, Davidsen TM, Beanan MJ, Deboy RT, Daugherty SC, Brinkac LM, Madupu R, Dodson RJ, Khouri HM, Lee KH, Carty HA, Scanlan D, Heinzen RA, Thompson HA, Samuel JE, Fraser CM, Heidelberg JF. 2003. Complete genome sequence of the Q-fever pathogen *Coxiella burnetii*. *Proc Natl Acad Sci U S A* **100**:5455–5460. doi:10.1073/pnas.0931379100

Sjödin A, Svensson K, Öhrman C, Ahlinder J, Lindgren P, Duodu S, Johansson A, Colquhoun DJ, Larsson P, Forsman M. 2012. Genome characterisation of the genus *Francisella* reveals insight into similar evolutionary paths in pathogens of mammals and fish. *BMC Genomics* **13**. doi:10.1186/1471-2164-13-268

Smith TA, Driscoll T, Gillespie JJ, Raghavan R. 2015. A *Coxiella*-like endosymbiontis a potential vitamin source for the lone star tick. *Genome Biol Evol* **7**:831–838. doi:10.1093/gbe/evv016

Szigeti A, Kreizinger Z, Hornok S, Abichu G, Gyuranecz M. 2014. Detection of *Francisella*-like endosymbiont in *Hyalomma rufipes* from Ethiopia. *Ticks Tick Borne Dis* **5**:818–820. doi:10.1016/j.ttbdis.2014.06.002

Visser ES, McGuire TC, Palmer GH, Davis WC, Shkap V, Pipano E, Knowles DP. 1992. The

bioRxiv preprint doi: https://doi.org/10.1101/2021.10.12.464044; this version posted October 13, 2021. The copyright holder for this preprint (which was not certified by peer review) is the author/funder, who has granted bioRxiv a license to display the preprint in perpetuity. It is made available under aCC-BY 4.0 International license.

Anaplasma marginale msp5 gene encodes a 19-kilodalton protein conserved in all recognized *Anaplasma* species. *Infect Immun* **60**:5139–5144. doi:10.1128/iai.60.12.5139-5144.1992

Wang Y, Mao L, Sun Y, Wang Z, Zhang Jiayong, Zhang Jibo, Peng Y, Xia L. 2018. A novel *Francisella*-like endosymbiont in *Haemaphysalis longicornis* and *Hyalomma asiaticum*, China. *Vector-Borne Zoonotic Dis* **18**:669–676. doi:10.1089/vbz.2017.2252